



# Attosecond Coherent X-ray Stimulated Raman (CXRS) Spectroscopy

Shaul Mukamel Daniel Healion

Haitao Wang

University of California, Irvine

Kavli Institute

August 2 ,2010

# Heterodyne-Detected

## (Stimulated) Four Wave Mixing

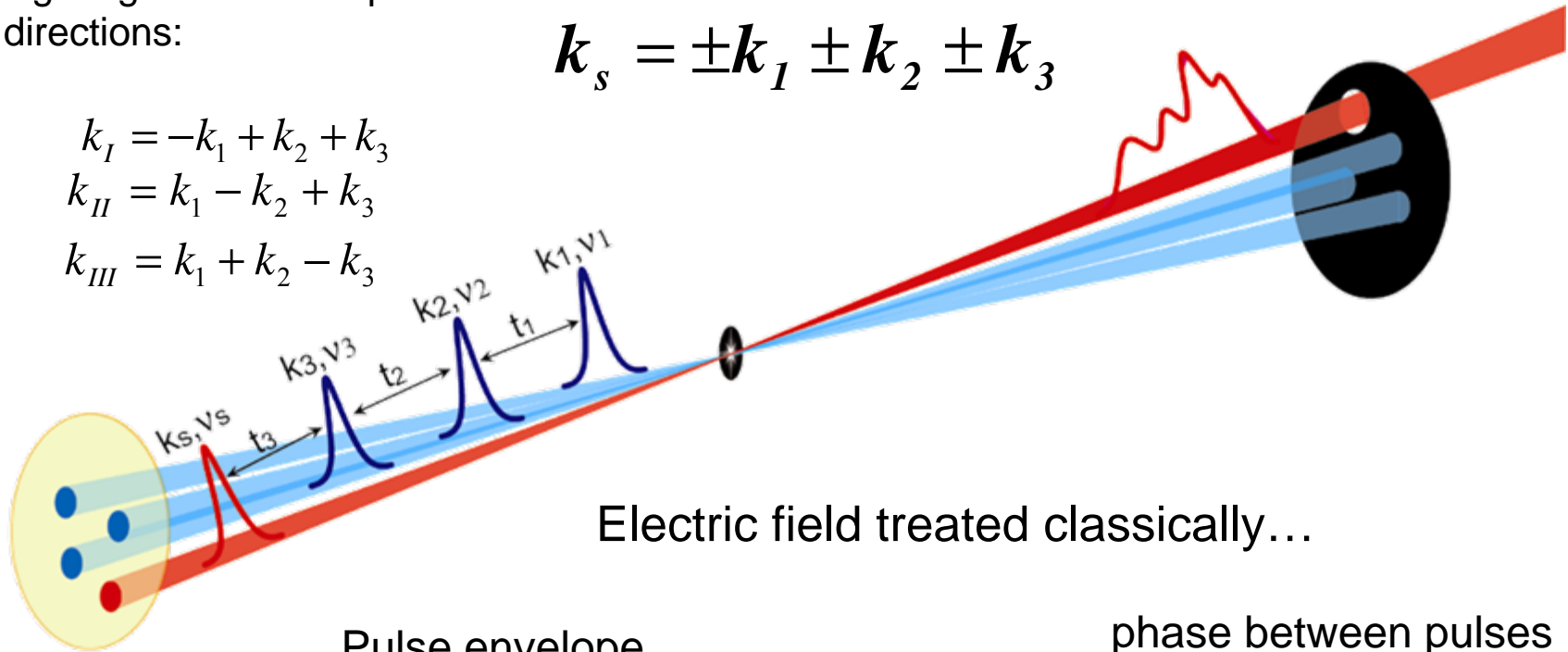
signal generated in specific directions:

$$k_s = \pm k_1 \pm k_2 \pm k_3$$

$$k_I = -k_1 + k_2 + k_3$$

$$k_{II} = k_1 - k_2 + k_3$$

$$k_{III} = k_1 + k_2 - k_3$$



Electric field treated classically...

Pulse envelope

phase between pulses

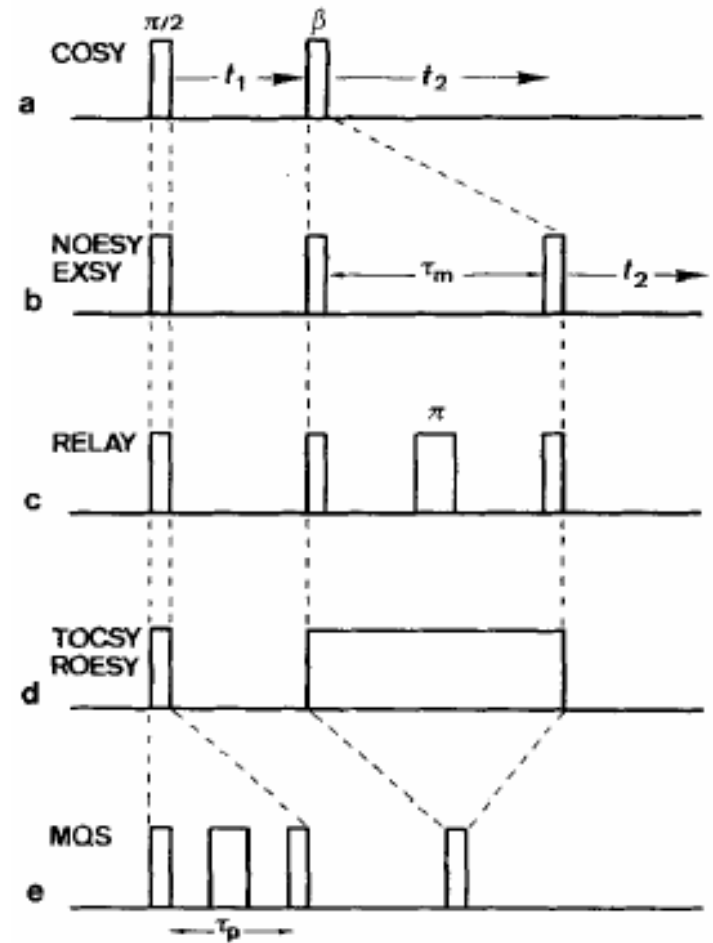
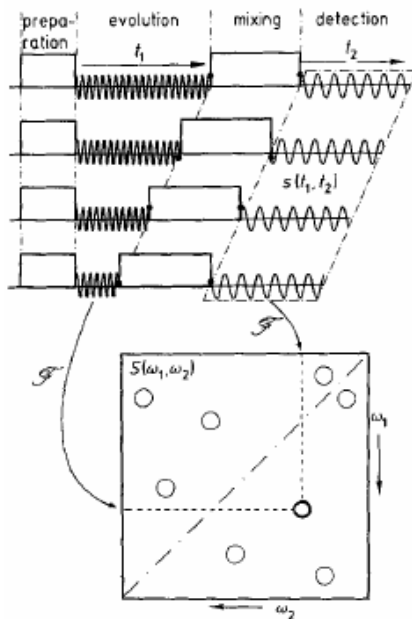
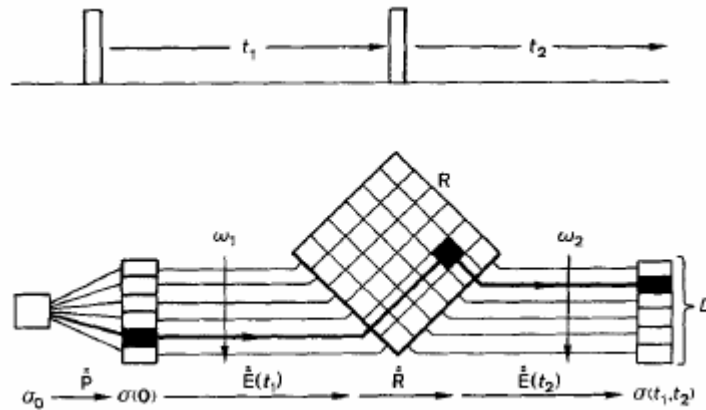
$$\mathbf{E}(\mathbf{r}, \tau) = \sum_{j=1}^4 \sum_v E_{jv}(\tau - \bar{\tau}_j) \exp[ik_j r - i\bar{\omega}_j(\tau - \bar{\tau}_j) - i\varphi_{jv}(\tau - \bar{\tau}_j)] + c.c.,$$

pulse #

polarization

...induces a polarization in the material

# 2D NMR Spectroscopy



# ANGEWANDTE CHEMIE

Volume 31 · Number 7

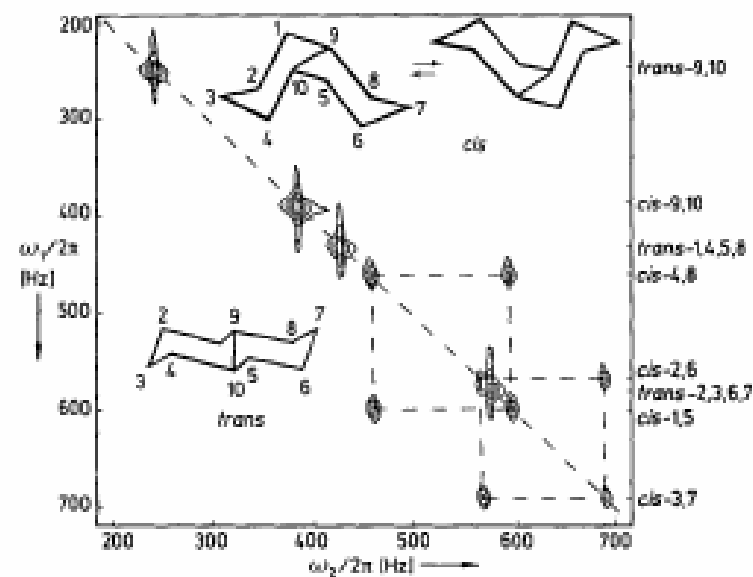
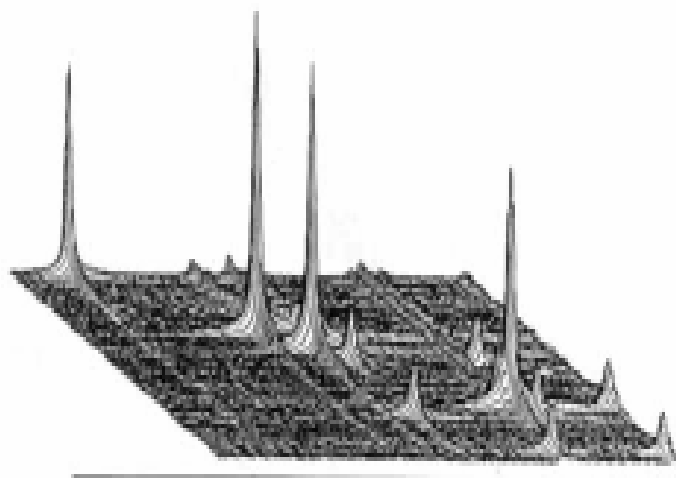
July 1992

Pages 805–930

International Edition in English

## Nuclear Magnetic Resonance Fourier Transform Spectroscopy (Nobel Lecture)\*\*

By Richard R. Ernst\*



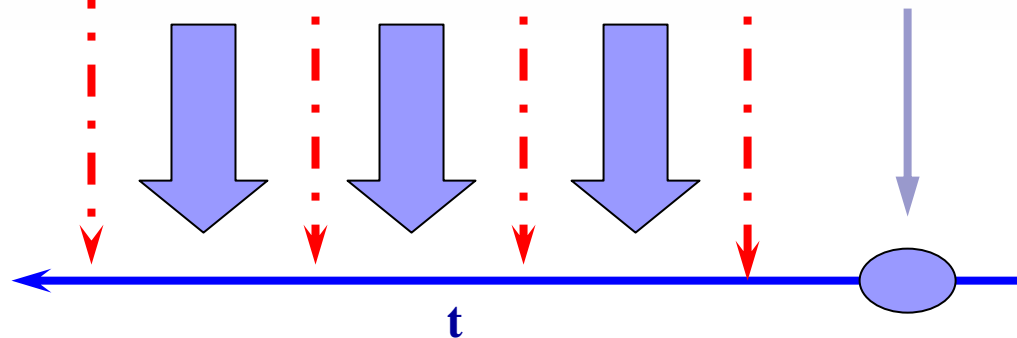
# The Nonlinear Response Functions

$$P(\mathbf{r}, t) = P^{(1)}(\mathbf{r}, t) + P^{(2)}(\mathbf{r}, t) + P^{(3)}(\mathbf{r}, t) + \dots$$

Nonlinear polarization  $P^{(n)}(\mathbf{r}, t) \equiv \langle\langle V | \rho^{(n)}(t) \rangle\rangle \equiv Tr[V \rho^{(n)}(t)]$

$$P^{(n)}(\mathbf{r}, t) = \int_0^\infty dt_n \int_0^\infty dt_{n-1} \dots \int_0^\infty dt_1 S^{(n)}(t_n, t_{n-1}, \dots, t_1) \\ \times E(\mathbf{r}, t - t_n) E(\mathbf{r}, t - t_n - t_{n-1}) \dots E(\mathbf{r}, t - t_n - t_{n-1} \dots - t_1),$$

$$S^{(3)}(t_3, t_2, t_1) = \left(\frac{i}{\hbar}\right)^3 \langle\langle V | \mathcal{G}(t_3) \mathcal{V} \mathcal{G}(t_2) \mathcal{V} \mathcal{G}(t_1) \mathcal{V} | \rho(-\infty) \rangle\rangle$$



# Two-dimensional correlation plots

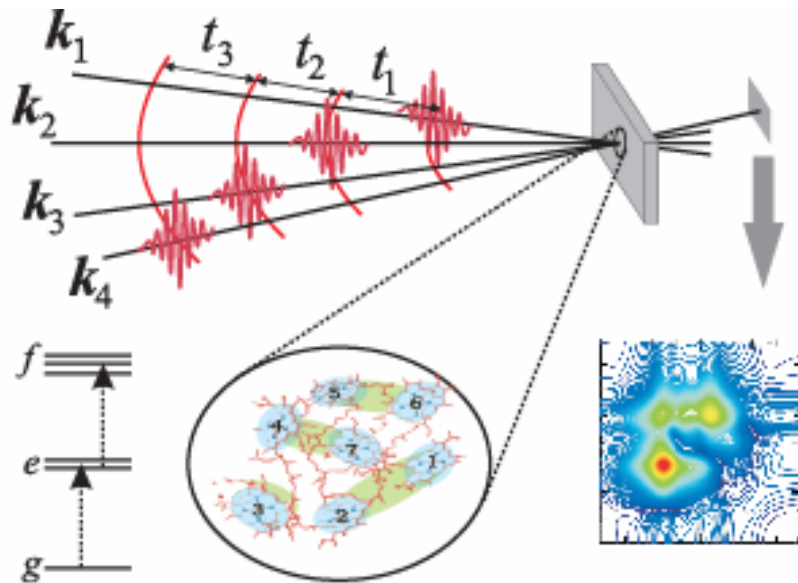
- Double Fourier transform:

$$S_I(\Omega_1, t_2, \Omega_3) = \int_0^\infty dt_3 \int_0^\infty dt_1 e^{i\Omega_1 t_1 + i\Omega_3 t_3} S(t_1, t_2, t_3)$$

$$S_{III}(t_1, \Omega_2, \Omega_3) = \int_0^\infty dt_3 \int_0^\infty dt_2 e^{i\Omega_2 t_2 + i\Omega_3 t_3} S(t_1, t_2, t_3)$$

- Particularly useful for displaying structural information, in analogy with 2D NMR
- Ultrafast (50 fs) time resolution
- Probe intra- and intermolecular interactions
- Spreading transitions in multiple dimensions
- Lineshapes give environment fluctuations

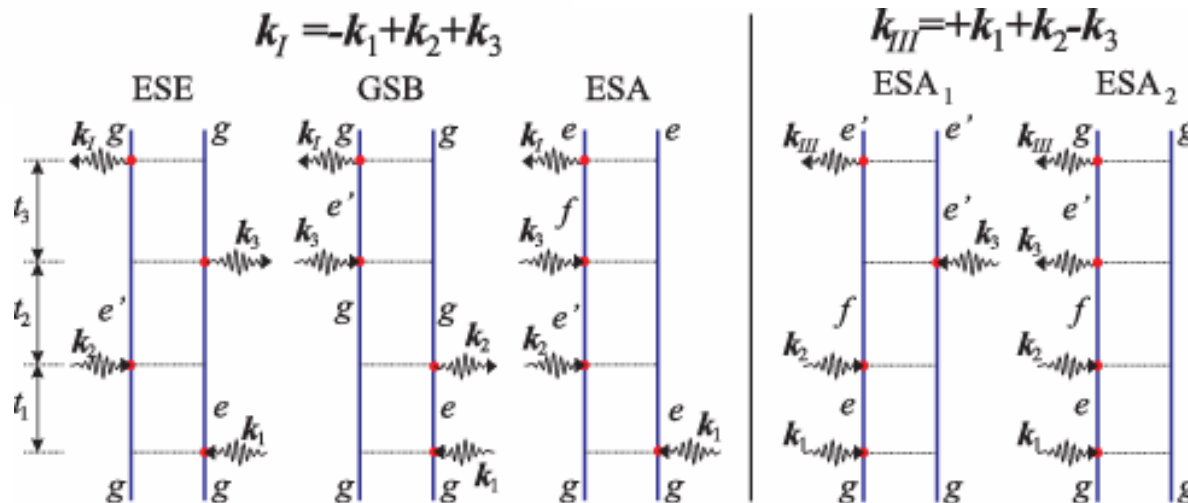
# The scheme of the four-wave-mixing experiment



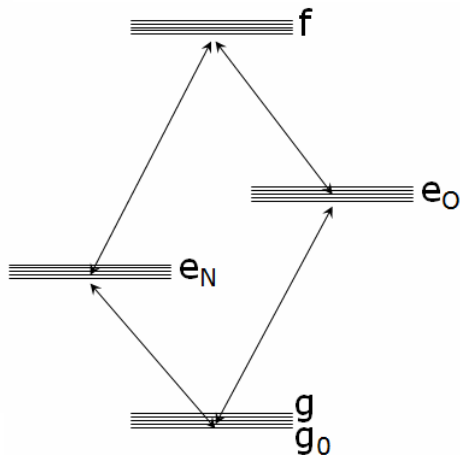
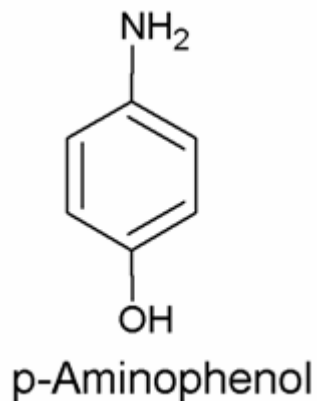
- The delay times between the pulses are the experiment parameters.
- Fourier transformations of signals with respect to time delays generate multidimensional spectrograms.

Generic three-band model

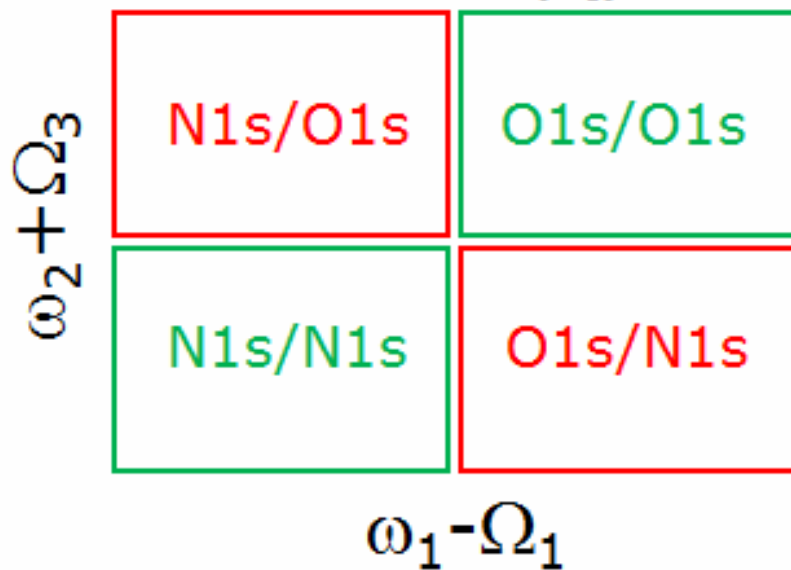
Feynman diagrams



# Simulated 2DXCS signal of para-aminophenol

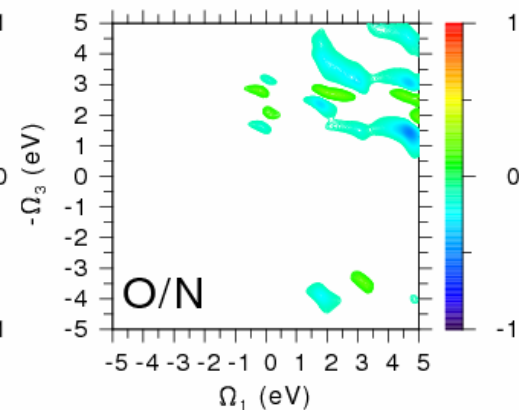
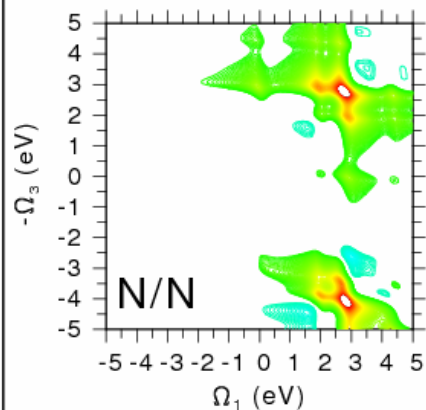
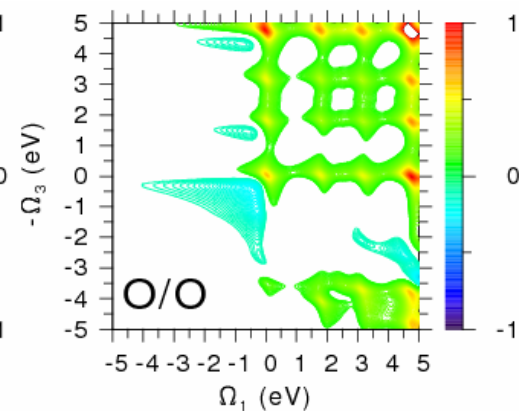
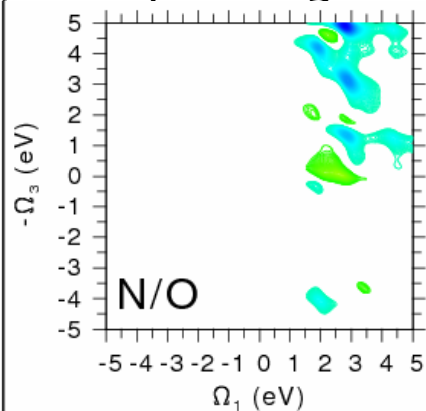


2DXCS ( $k_I$ )



Simulation:

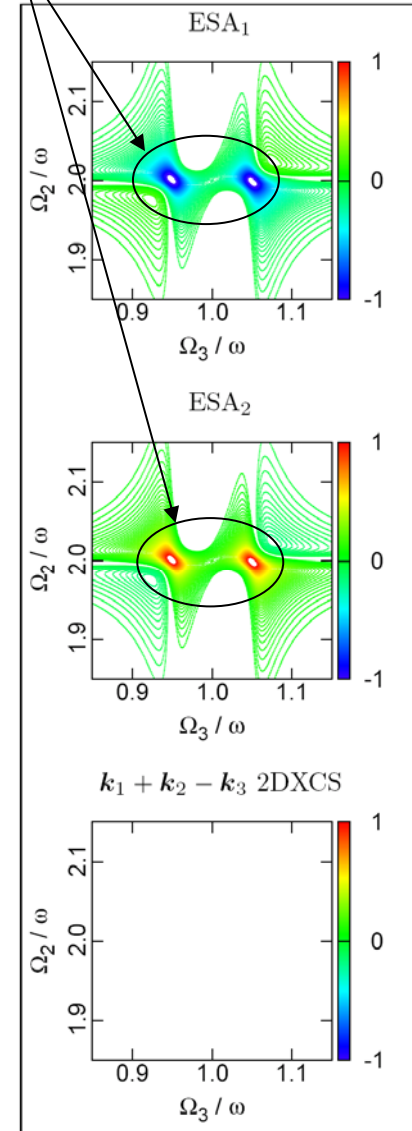
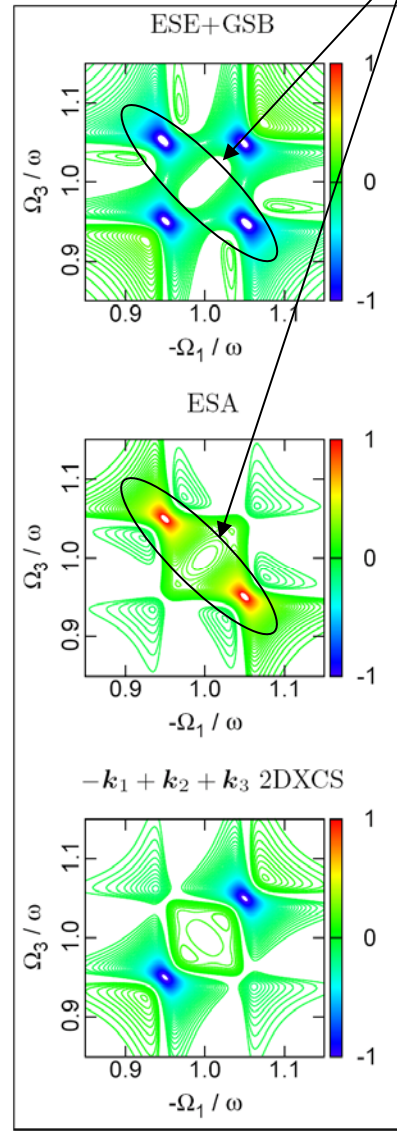
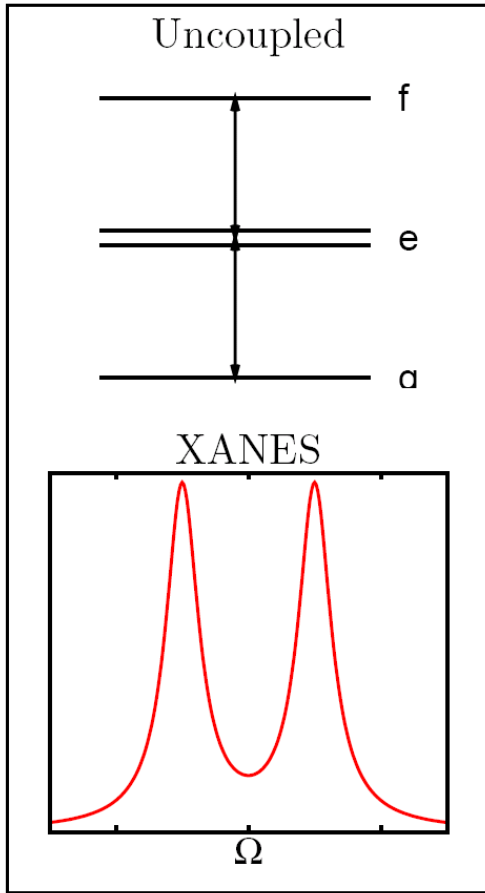
- Equivalent-core approx.
- B3LYP/6-311G\*\* orbitals
- Bandwidth: 6 eV
- Dephasing: 0.3 eV





# $k_I$ and $k_{III}$ of an uncoupled system

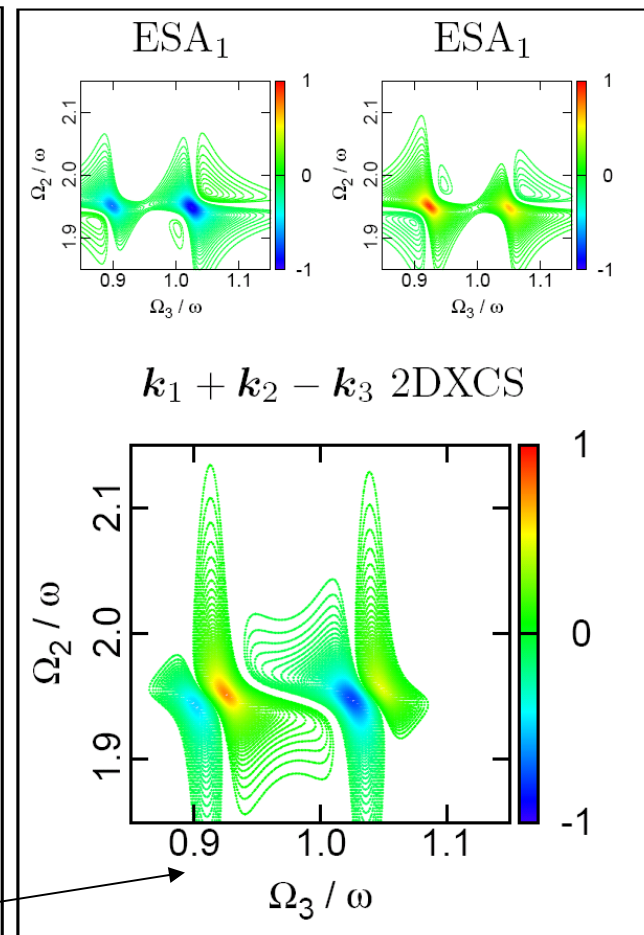
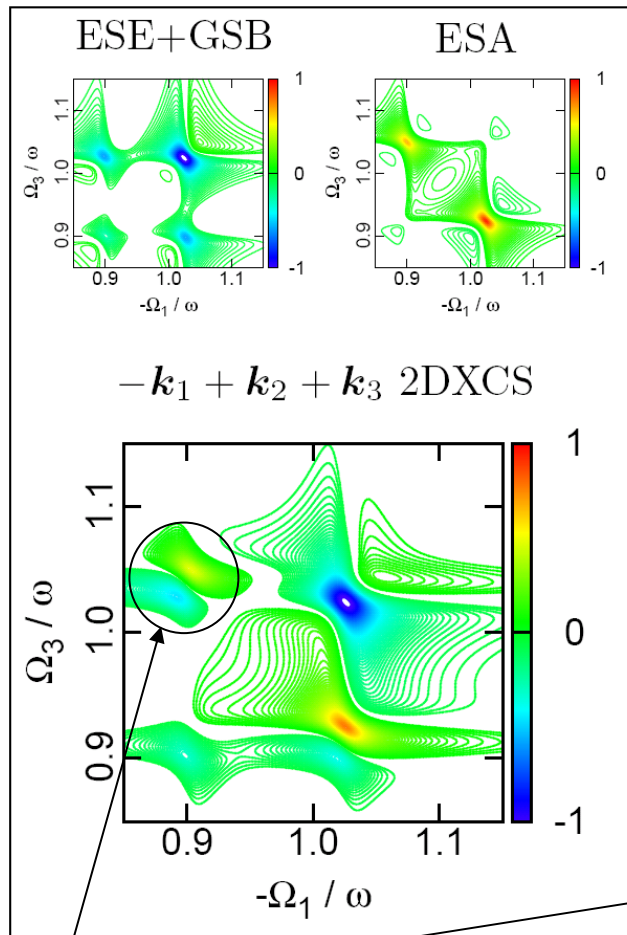
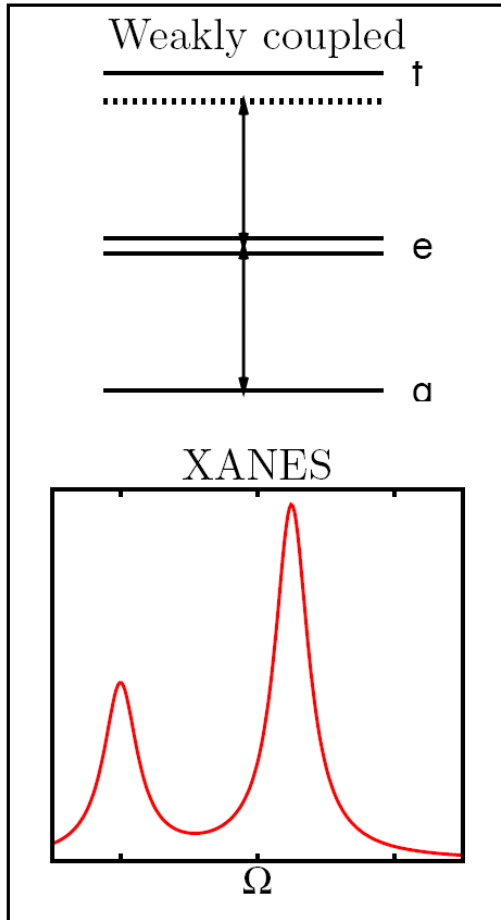
opposite signs



off diagonal peaks in  
photon echo cancel exactly

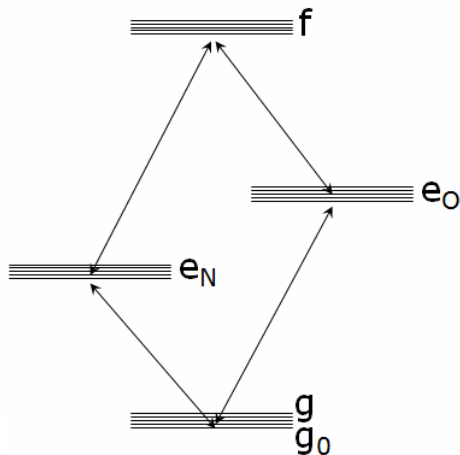
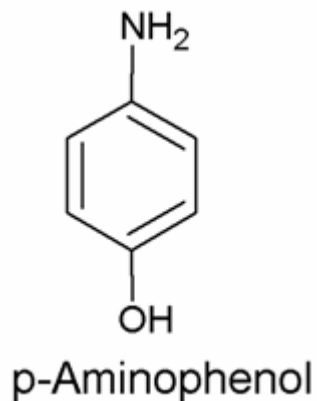
...as does the  $k_{III}$   
signal.

# $k_I$ and $k_{III}$ of a coupled system

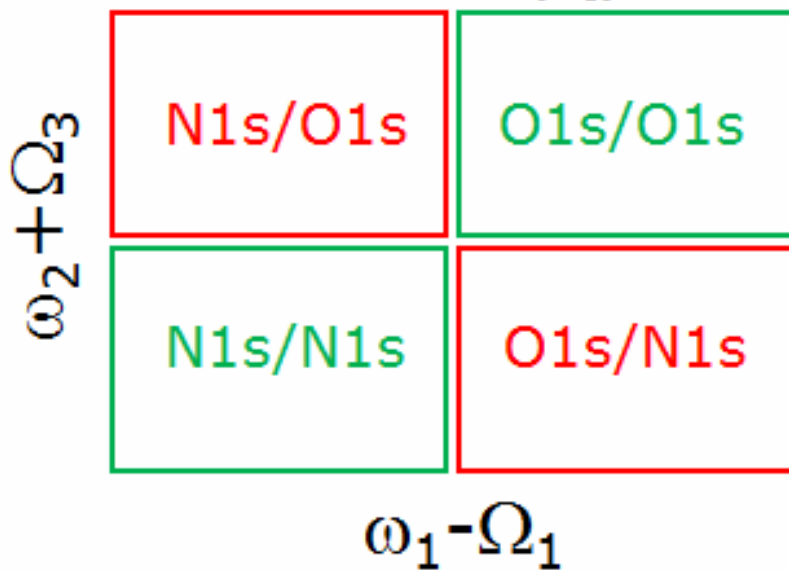


off-diagonal cross-peaks in  $k_I$  and a non-vanishing  $k_{III}$  signal are signatures of core-hole coupling

# Simulated 2DXCS signal of para-aminophenol

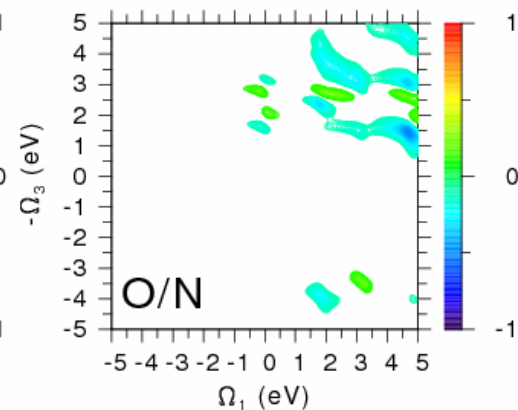
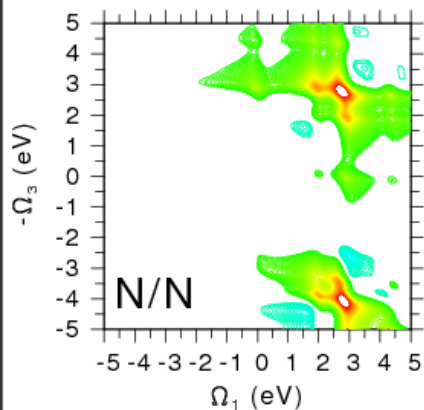
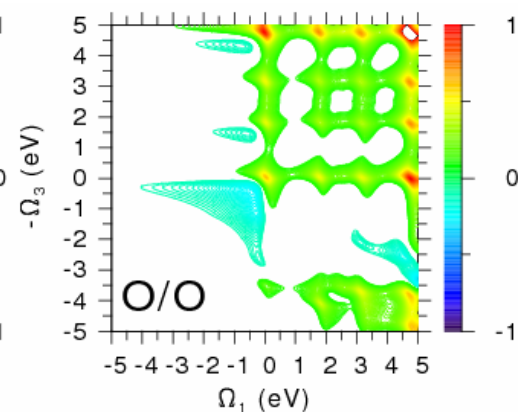
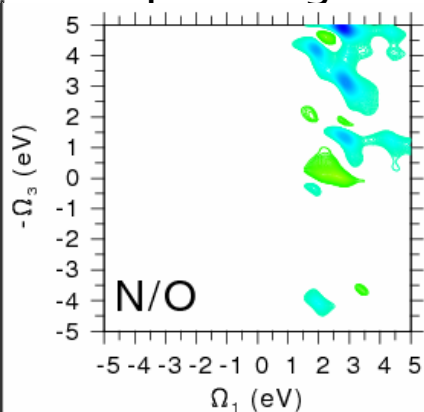


2DXCS ( $k_I$ )

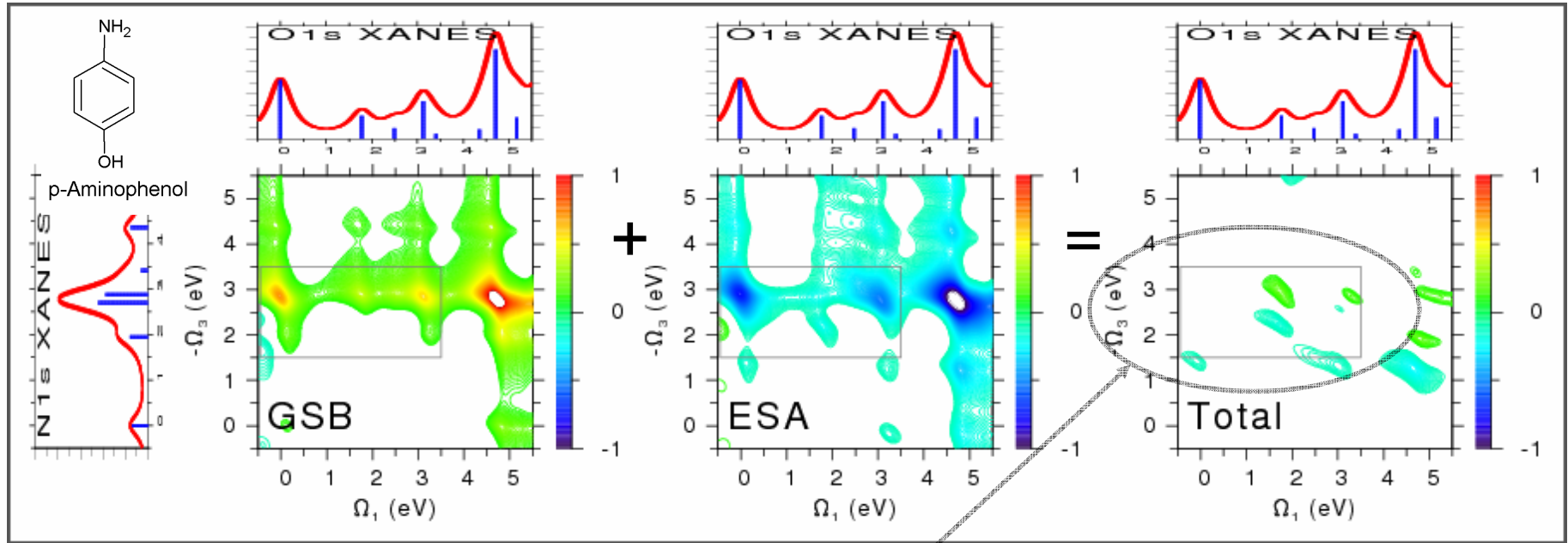


Simulation:

- Equivalent-core approx.
- B3LYP/6-311G\*\* orbitals
- Bandwidth: 6 eV
- Dephasing: 0.3 eV

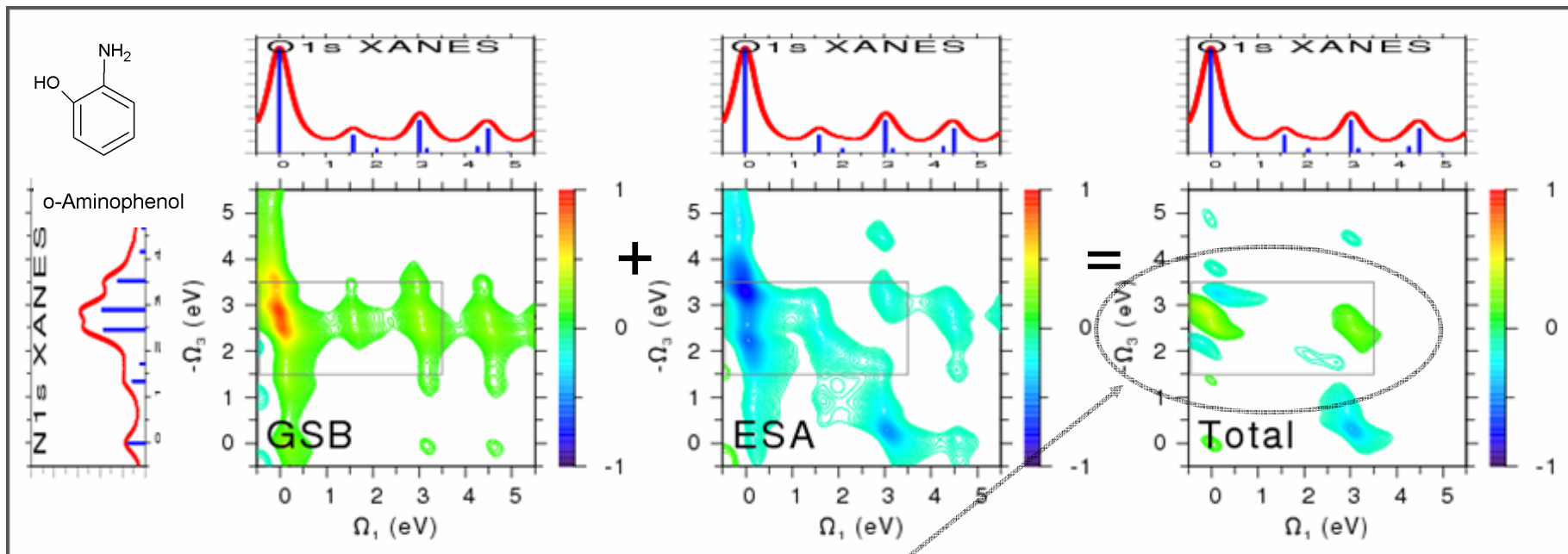


# Simulated O1s/N1s 2DXCS cross peak of para-aminophenol



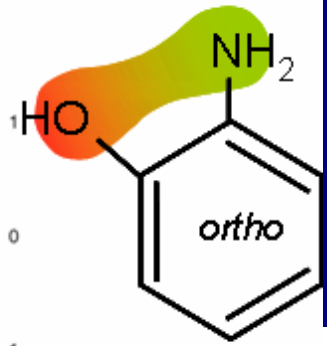
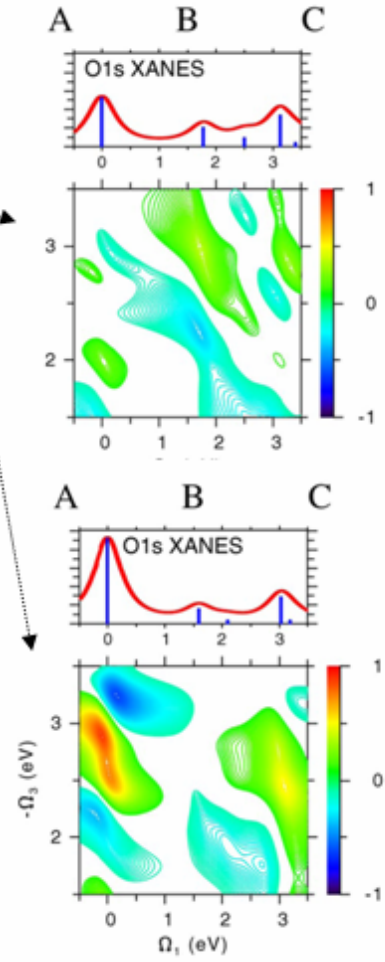
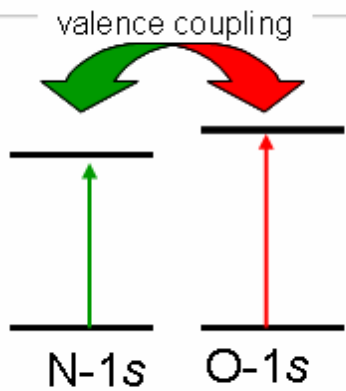
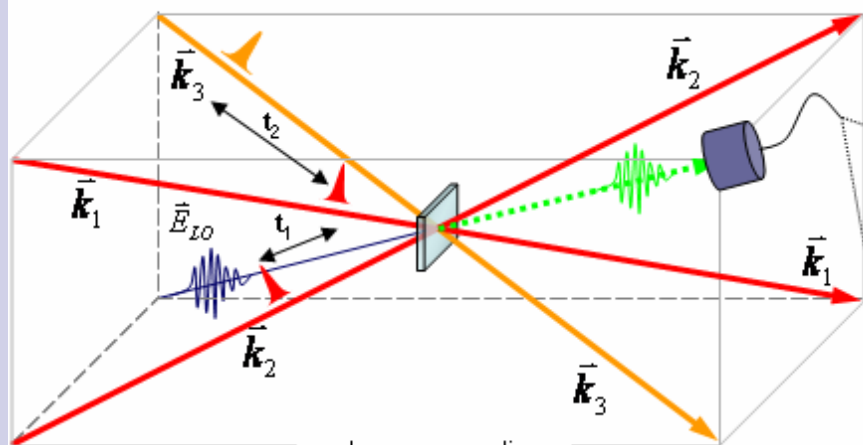
- In the para isomer, interactions between N1s and O1s core transitions are weak  $\Rightarrow$  cross peaks are weak despite the strong GSB and ESA components

# Simulated O1s/N1s 2DXCS cross peak of ortho-aminophenol

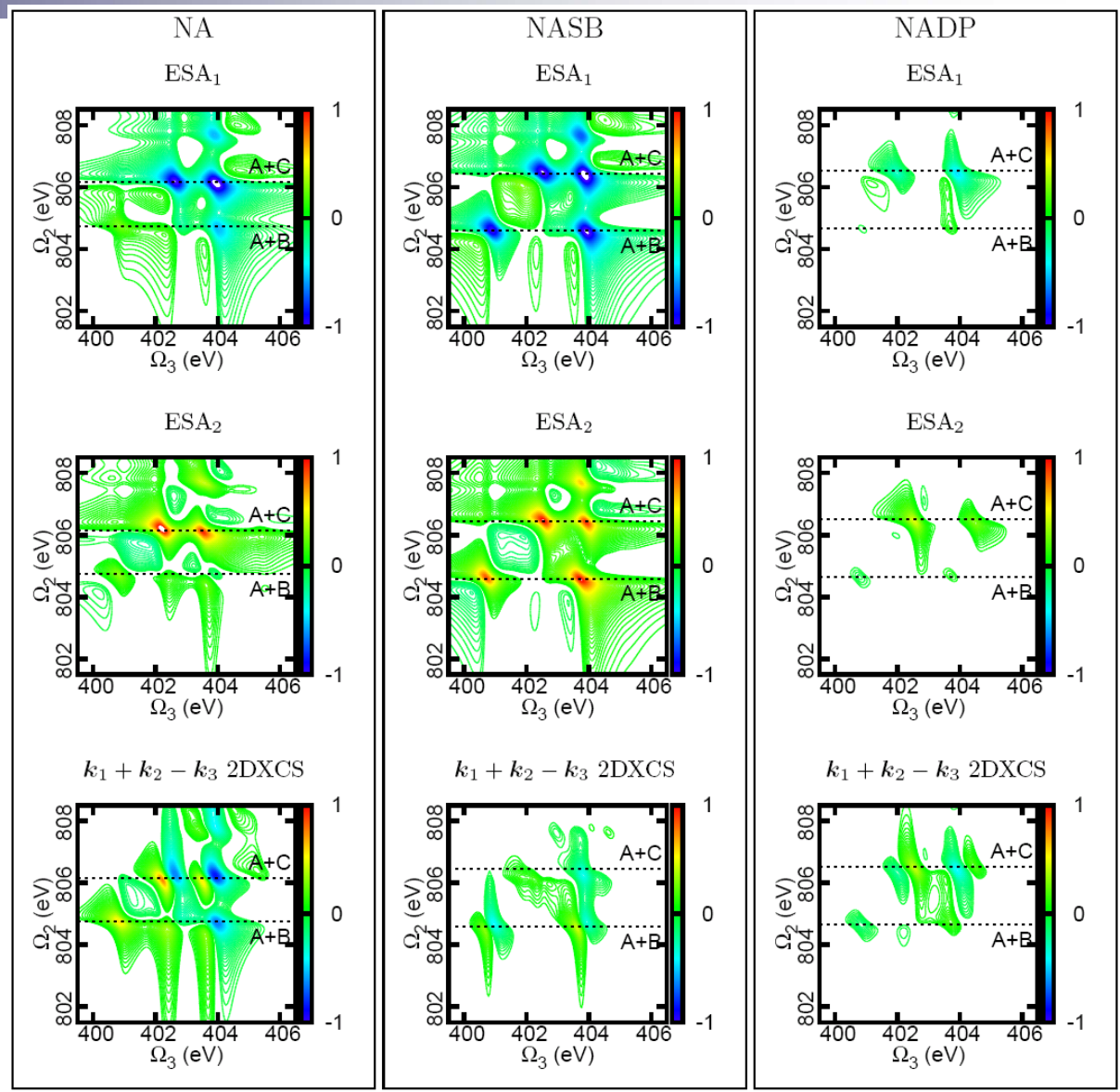
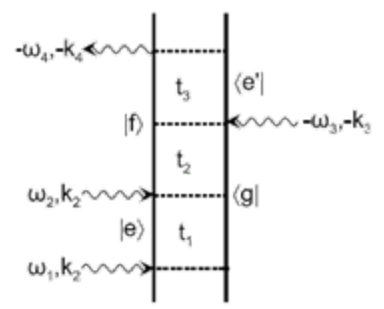
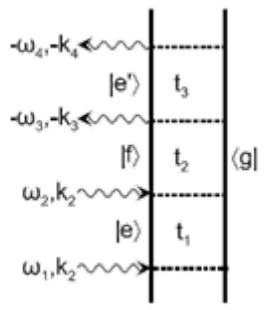
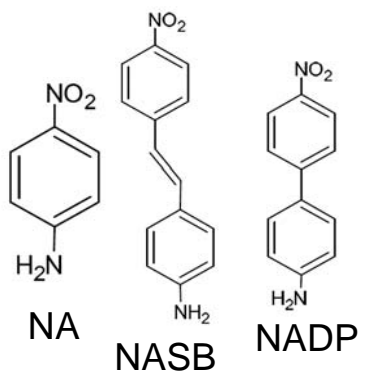


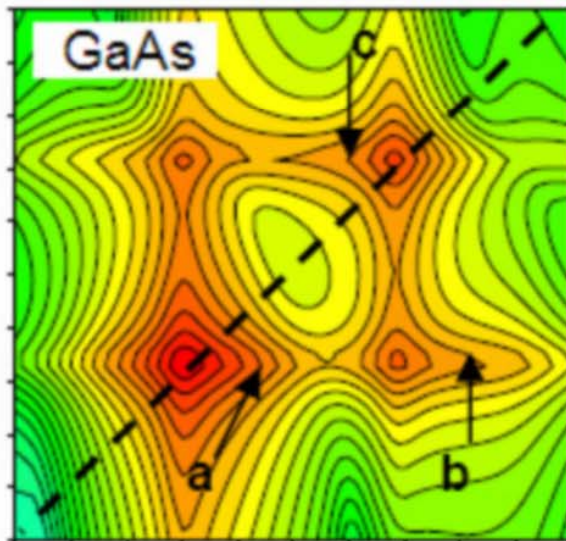
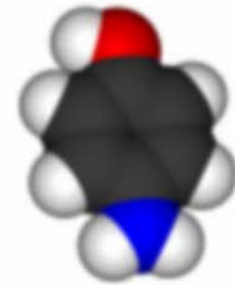
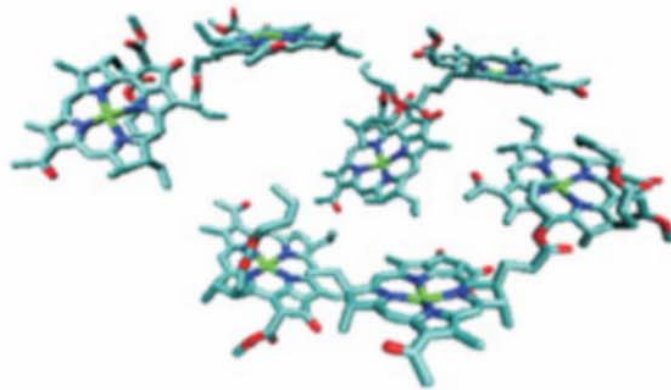
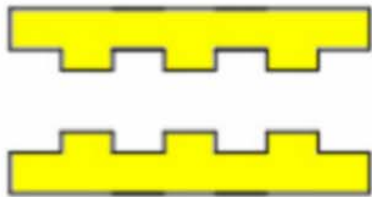
- In the ortho isomer, interactions between the N1s and O1s are stronger  $\Rightarrow$  different peak pattern with stronger cross peaks

-Unlike XANES, 2DXCS cross peaks are sensitive to the relative position of the O and N atoms

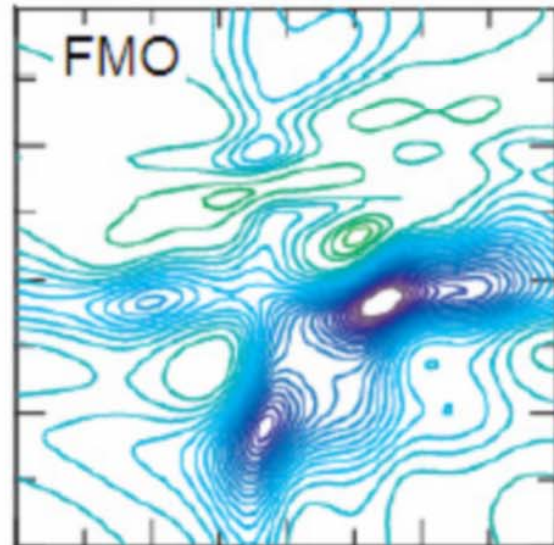


**Left:** Proposed four-wave mixing of ultrashort x-ray pulses resonant with the O-1s and N-1s levels; **Middle:** theoretically predicted two-dimensional spectra the lower of which exhibits the coupling of excitations on the oxygen with those of the nitrogen in para and ortho-aminophenol molecules at right [from S. Mukamel].

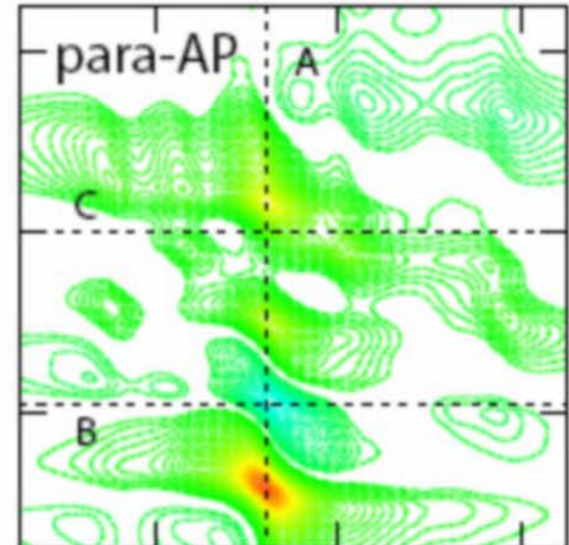




GaAs  
Wannier excitons  
(meV)



FMO  
Frenkel excitons  
(0.1 eV)

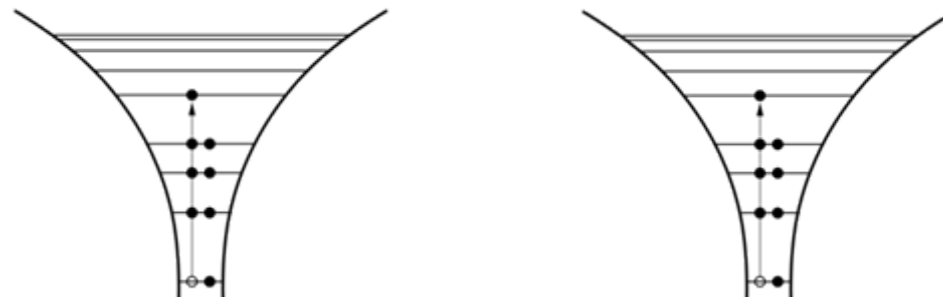
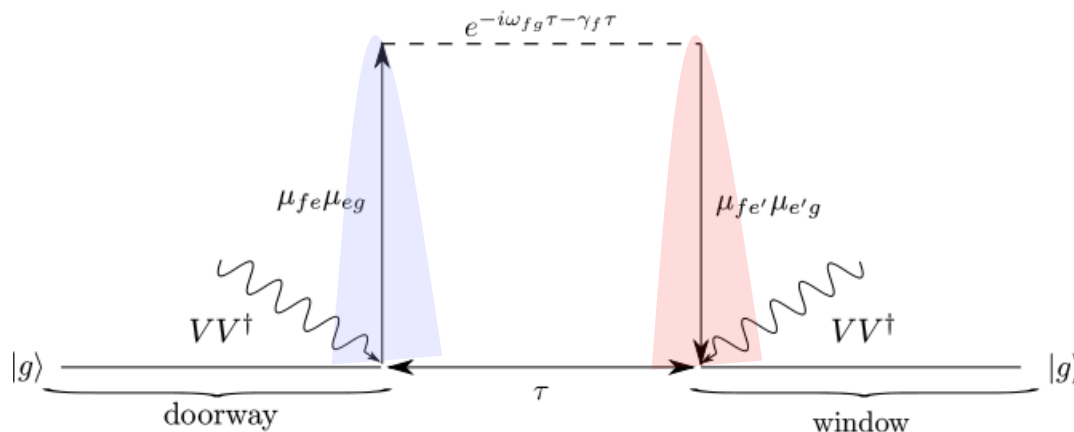
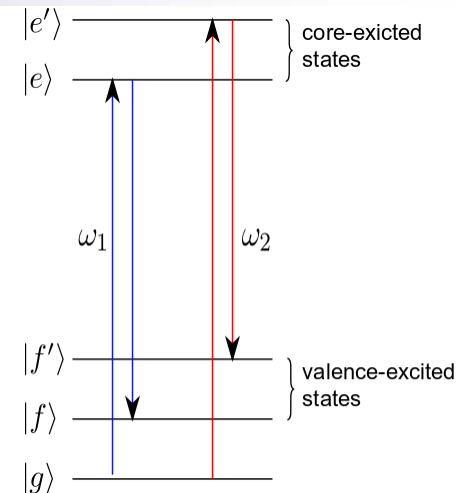
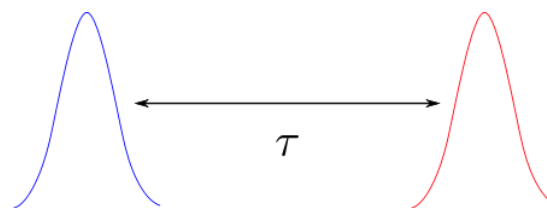


para-AP  
Core excitons  
(eV)



# Coherent X-ray Stimulated Raman Spectroscopy (CXRS)

- Two well-separated pulses with Gaussian envelopes
- Each pulse interacts with the molecule twice, to create a valence electronic wave packet. No phase control is needed.
- Delay time between pulses (fs~ps) is not limited by core-hole lifetime.

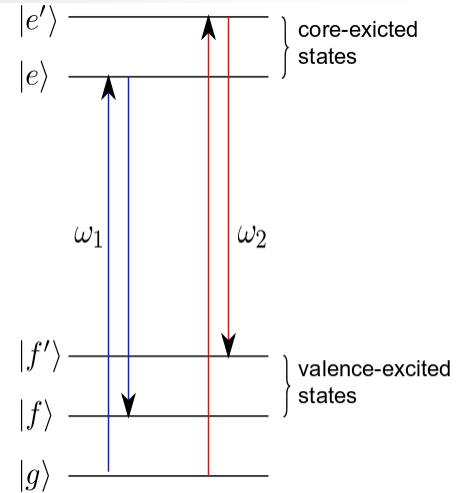


Schweigert, Mukamel; PRA, 76 0125041 (2007)

Harbola, Mukamel; PRB 79, 085108 (2009)

# Hamiltonian

$$\hat{H}_{total} = \hat{H}_{mol} + \hat{H}_{int}$$



$$\hat{H}_{mol} = \sum_i \epsilon_i c_i^\dagger c_i + \frac{1}{2} \sum_{ijkl} V_{ijkl} c_i^\dagger c_j^\dagger c_l c_k$$

orbital energies

Coulomb scattering

$$V_{ijkl} = \int d\vec{r} \int d\vec{r}' \frac{\phi_i^*(\vec{r}) \phi_j^*(\vec{r}) \phi_k(\vec{r}') \phi_l(\vec{r}')}{|\vec{r} - \vec{r}'|}$$

molecular orbitals

$c_i^\dagger, c_i$  ← Fermi operators

two X-ray pulses

$$\mathcal{E}(\vec{r}, t) = \sum_{j=1,2} E_j(\vec{r}, t) + E_j^*(\vec{r}, t)$$

pulse duration

with gaussian  
pulse envelopes

central frequency

$$E_j(\vec{r}, t) = \frac{1}{\sigma_j \sqrt{2\pi}} e^{-t^2 / 2\sigma_j^2} e^{i\vec{k}_j \cdot \vec{r} - i\omega_j t}$$

wave vector

in the frequency domain:

$$E(\vec{r}, \omega) = \sum_{j=1,2} E_j^+(\vec{r}, \omega) + E_j^-(\vec{r}, \omega)$$

$$E_j^\pm(\vec{r}, \omega) = \frac{\sigma_j}{\sqrt{2\pi}} e^{-(\omega \pm \omega_j)^2 \sigma_j^2 / 2} e^{\pm i\vec{k}_j \cdot \vec{r}}$$

# Closed-Time-Path Loop Diagrams

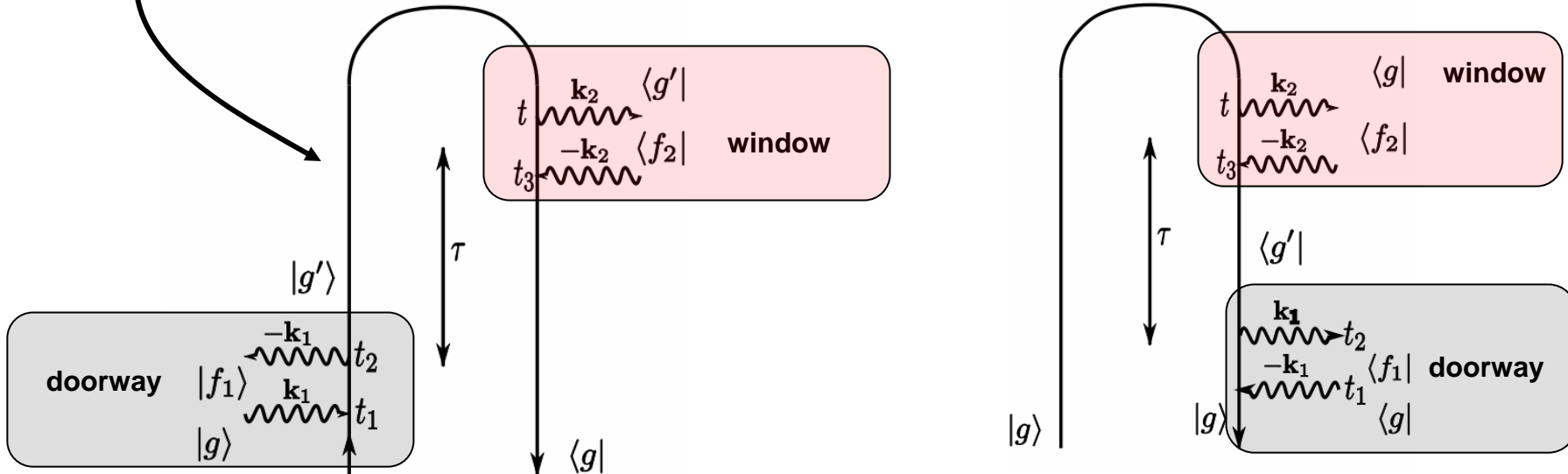
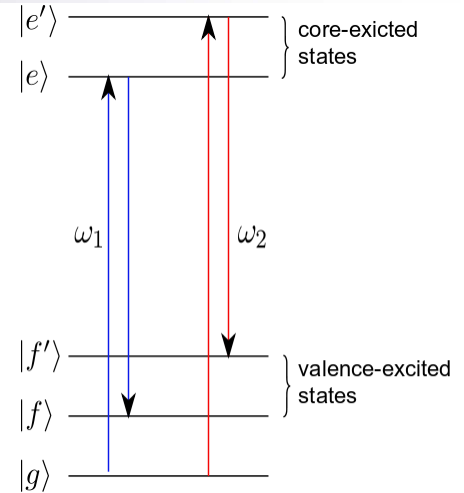
The stimulated Raman signal is a sum over two terms:

$$S_{SR}(\tau) = 2\text{Re} \int_{-\infty}^{\infty} dt \int_{-\infty}^t dt_3$$

$$\times \left[ \int_{-\infty}^{\infty} dt_2 \int_{-\infty}^{t_2} dt_1 \langle V(t_3) V^\dagger(t) V(t_2) V^\dagger(t_1) \rangle \right.$$

$$\left. + \int_{-\infty}^{\infty} dt_1 \int_{-\infty}^{t_1} dt_2 \langle V(t_2) V^\dagger(t_1) V(t_3) V^\dagger(t) \rangle \right]$$

$$E_2(t - \tau) E_2^*(t_3 - \tau) E_1^*(t_2) E_1(t_1)$$



# CXRS Signal: Doorway-Window Picture

A time-dependent overlap between valence electronic wavepackets

$$S_{SR}(\tau) = \text{Re} \sum_f W_f^* D_f e^{-i\omega_{fg}\tau - \gamma_f \tau}$$
$$= \text{Re} \langle W | D(\tau) \rangle$$

valence-excited  
state decay rate

$$|D(\tau)\rangle = \sum_f D_f e^{-i\omega_{fg}\tau - \gamma_f \tau} |f\rangle$$

doorway and window wave  
packets expanded in many-  
body valence-excited states

$$|W\rangle = \sum_f W_f |f\rangle$$

# CXRS Signal: Doorway and Window Wave Packets

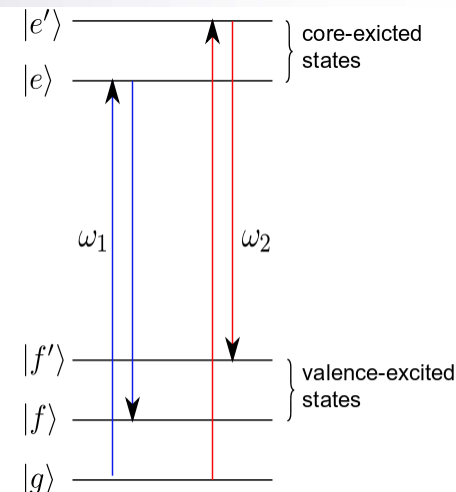
Two difficulties calculating the SOS expressions

$$D_f = \sum_e \mu_{fe} \mu_{eg} \int \frac{d\omega}{2\pi} \frac{E_1^*(\omega) E_1(\omega - \omega_{fg})}{\omega - \omega_{fg} - \omega_e + i\gamma_e}$$

(1) Matrix elements evaluated between states with different core occupations

$$W_f = \text{Im} \sum_{e'} \mu_{fe'} \mu_{e'g} \int \frac{d\omega}{2\pi} \frac{E_2^*(\omega) E_2(\omega - \omega_{fg})}{\omega - \omega_{fg} - \omega_{e'} + i\gamma_{e'}}$$

(2) Integration over electric field envelopes performed analytically



# Spontaneous Resonant inelastic x ray scattering Kramers-Heisenberg Expression

$$S_{\text{RIXS}}(\omega_1, \omega_2) = \sum_{ac} |A_{ca}(\omega_1)|^2 \delta(\omega_1 - \omega_2 - \omega_{ca})$$
$$A_{ca}(\omega_1) = \sum_e \frac{B_{ce} B_{ea}}{\omega_1 - \omega_{ea} + i\Gamma_{ea}}$$

- ★  $\omega_1$  and  $\omega_2$  are the incoming and outgoing modes
- ★  $a$  and  $c$  are valence N - electron ground and singly excited states
- ★  $B_{ea}$  and  $B_{ce}$  are matrix elements of dipole operator
- ★  $\Gamma$  is the inverse life - time of the excited state wave - packet

# Computation of Core-Excited States

- Deep core electrons are weakly correlated with other electrons.  
Large energy separation between core orbital space and valence orbital space.
- Strong orbital relaxation upon core-electronic excitations.  
Koopmans' theorem does not apply.

## Goals:

- Describe orbital relaxation.
- Describe different core-hole configurations: deep and shallow core-holes.
- Incorporate electron correlations, especially for shallow core-hole configurations.



# Core-Excited States: Equivalent-Core Approximation (ECA)

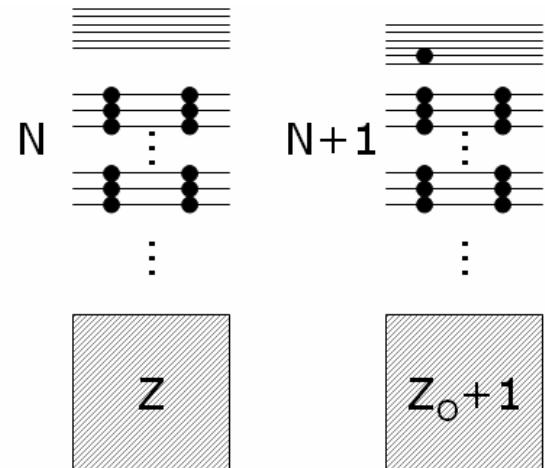
ECA( $Z+1$ ) approximation: Mimics the creation of the core hole by incrementing the nuclear charge and adding a valence electron

## Advantages:

- Number of electrons and nuclear configuration are standard input in existing electronic structure packages.
- Explicit treatment of core-hole is avoided.
- Double-core excitations are treated similarly.

## Limitations:

- Inherently incorrect spin symmetry — Modified ECA model by Cederbaum et al. JCP, 116:8723 (2002)
- Does not hold for shallow core holes



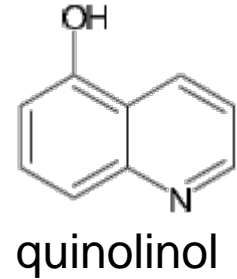
## References:

W. H. E. Schwarz and R. Buenker, Chem. Phys., 12:153 (1976)

# X-ray stimulated Raman spectroscopy of quinolinol (ECA)

All-x-ray resonant pump probe measurement

- pump prepares molecules either in ground/valence or core/core coherences
- core/core coherences decay rapidly ( $T_e \approx 10$  fs) due to the Auger ionization
- only Raman-type, GSB terms contribute for  $\tau > T_e$

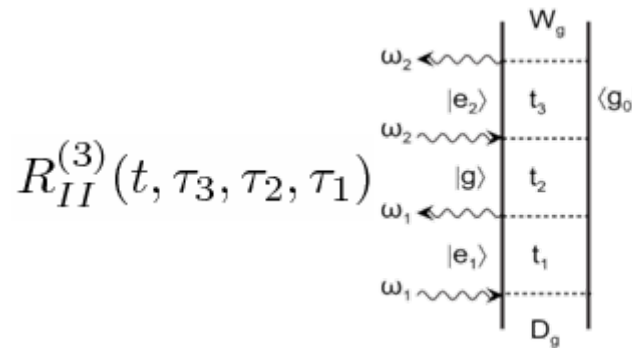
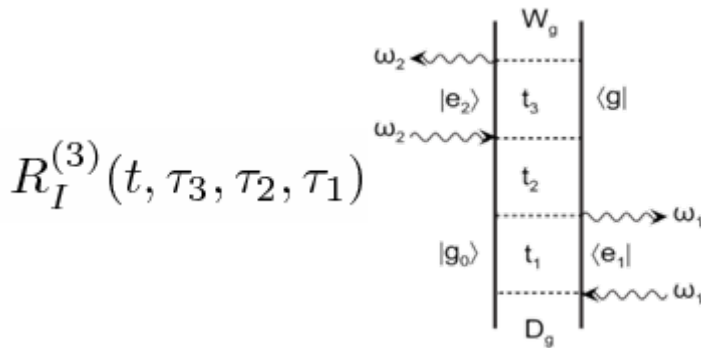
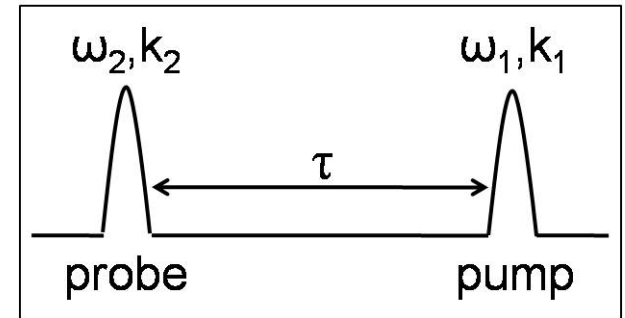


Stimulated Raman signal

$$S(\omega_1, \omega_2, \tau) = \text{Im} \int_{-\infty}^{\infty} dt \int_{-\infty}^t d\tau_3 \int_{-\infty}^{\tau_3} d\tau_2 \int_{-\infty}^{\tau_2} d\tau_1 [$$

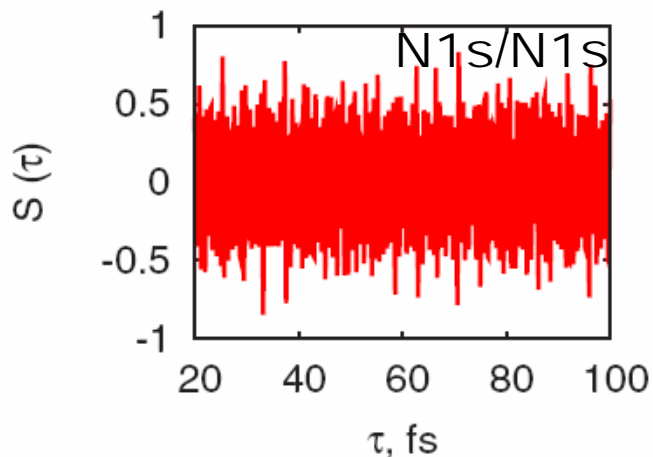
$$R_I^{(3)}(t, \tau_3, \tau_2, \tau_1) \mathcal{E}_2^*(t - \tau) \mathcal{E}_2(\tau_3 - \tau) \mathcal{E}_1(\tau_2) \mathcal{E}_1^*(\tau_1) e^{i\omega_2(t - \tau_3) - i\omega_1(\tau_2 - \tau_1)}$$

$$+ R_{II}^{(3)}(t, \tau_3, \tau_2, \tau_1) \mathcal{E}_2^*(t - \tau) \mathcal{E}_2(\tau_3 - \tau) \mathcal{E}_1^*(\tau_2) \mathcal{E}_1(\tau_1) e^{i\omega_2(t - \tau_3) + i\omega_1(\tau_2 - \tau_1)}]$$

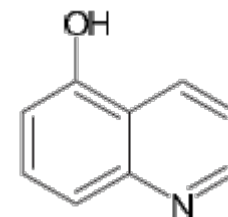
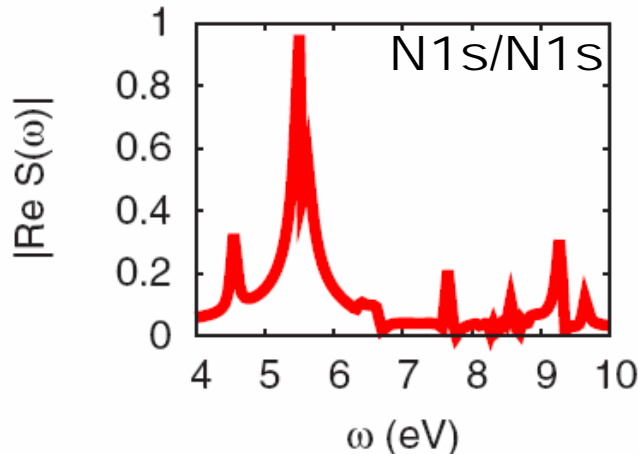


# X-ray stimulated Raman spectroscopy of quinolinol

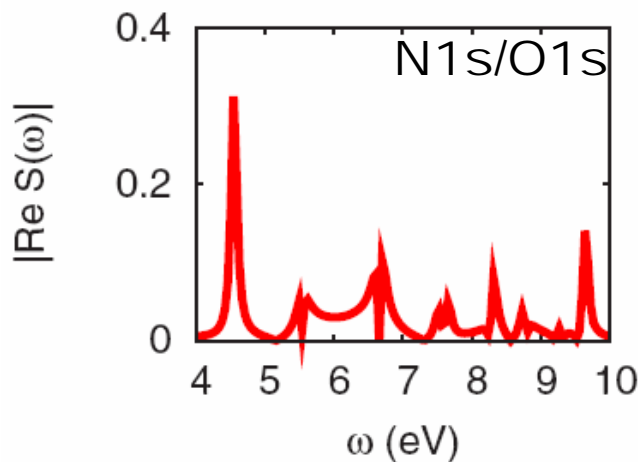
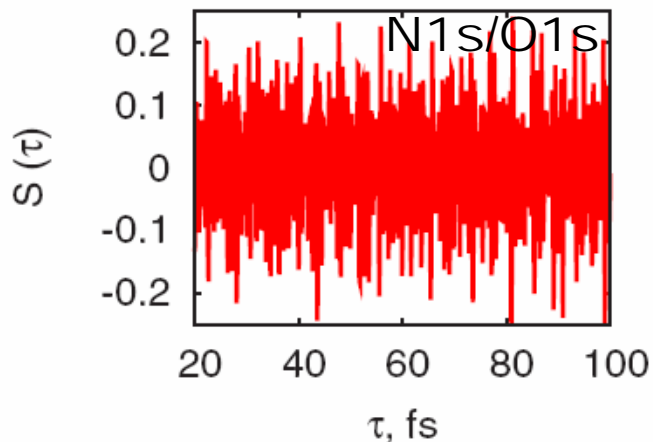
Stimulated Raman signal,  
 $10 < \tau < 100$  fs



Real part of the Fourier transform w.r.t.  $\tau$



Core and valence transitions:  
Singly-substituted KS determinants in the equivalent-core approximation, B3LYP/6-311G\*\*



-Peaks in the Fourier transform correspond to the energies of valence excited states contributing to the pump-induced wavepacket

# Core-Excited States: Static-Exchange (STEX) Approximation

Step 1: Optimize ground state of the neutral molecule at Hartree-Fock (HF) level.

$$|\Psi_{ref}^N\rangle_0 \text{ with energy } E_0^N$$

For valence-excited states using configuration interaction singles (CIS) wave function using HF orbitals. (Not a good approximation for core-excited states)

$$|\Psi_{i \rightarrow a}^N\rangle = \sum_{ia} C_i^a c_a^\dagger c_i |\Psi_{ref}^N\rangle_0$$

Step 2: Instead, for core-excited state, create ionized state with an electron ejected from a specific core orbital.

$$|\Psi_{n_\sigma}^{N-1}\rangle_0 = c_{n_\sigma} |\Psi_{ref}^N\rangle_0$$

↖ core orbital

References:

H. Ågren, Theor. Chem. Acc, 97:14 (1997)

W. Hunt and W. Goddard, CPL, 3:414 (1969)

# Core-Excited States: Static-Exchange (STEX) Approximation

Step 3: Optimize occupied orbitals of the target ionized state with occupation number fixed.

$$|\Psi_{n_\sigma}^{N-1}\rangle_0 \longrightarrow |\Psi_{n_\sigma}^{N-1}\rangle_{rel} \text{ with energy } E_n^{N-1}$$

Step 4: Optimize unoccupied orbitals by the static-exchange Hamiltonian holding occupied orbitals fixed.

$$\hat{F}_n^{STEX} = \hat{F} - \hat{J}_n + 2\hat{K}_n$$

$$\hat{F}_n^{STEX} \psi_a = \varepsilon_a \psi_a \longleftarrow \text{excited orbital}$$

Step 5: Add an electron to one of the optimized unoccupied orbitals, and construct the final core-excited state as an anti-symmetrized product of the target ionized state and the excited orbital.

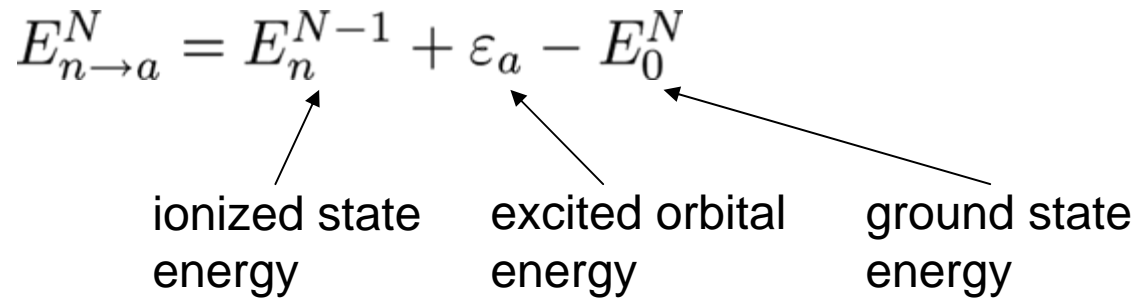
$$|\Psi_{n \rightarrow a}^N\rangle_{rel} = \frac{1}{\sqrt{2}} \left( c_{a_\alpha}^\dagger |\Psi_{n_\alpha}^{N-1}\rangle_{rel} + c_{a_\beta}^\dagger |\Psi_{n_\beta}^{N-1}\rangle_{rel} \right)$$

# Core-Excited States: Static-Exchange (STEX) Approximation

Step 6: Excitation energy of core-excited state :

$$E_{n \rightarrow a}^N = E_n^{N-1} + \varepsilon_a - E_0^N$$

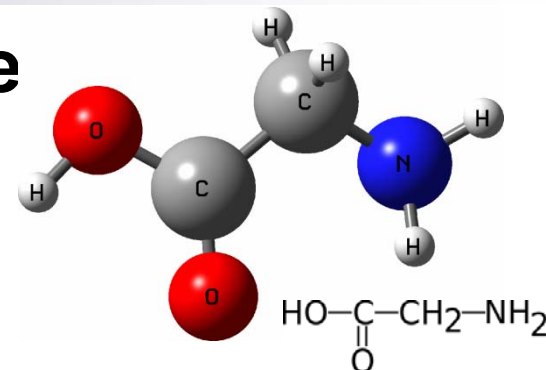
ionized state energy      excited orbital energy      ground state energy



Advantages:

- Correct spin symmetry (singlet -> singlet)
- Occupied and unoccupied orbital relaxation
- Can describe different core-hole configurations
- Electron correlation effects can be incorporated by using more accurate wave functions (e.g. CISD ... )

# Application to Glycine



- Geometry optimized at B3LYP/6-311G\*\* level.
- Energies and transition dipole moments calculated with 6-311G\*\* basis set.
- Valence-excited states described at CIS level. In molecular orbital basis:

$$\begin{cases} |D(\tau)\rangle = \sum_f D_f e^{-i\omega_{fg}\tau - \gamma_f\tau} |f\rangle \\ |W\rangle = \sum_f W_f |f\rangle \end{cases} \Rightarrow$$

$$\begin{cases} |D(\tau)\rangle = \sum_{f,ia} e^{-i\omega_{fg}\tau - \gamma_f\tau} D_{f;ia} c_a^\dagger c_i |g\rangle \\ |W\rangle = \sum_{f,ia} W_{f;ia} c_a^\dagger c_i |g\rangle \end{cases}$$

Linewidth:

$$\gamma_N = 0.085\text{eV}$$

$$\gamma_O = 0.10\text{eV}$$

$$\gamma_f = 0.05\text{eV}$$

Pulse duration:

$$\sigma_j = 77\text{as} (1/\sigma_j \simeq 10\text{eV})$$

Simulation time:

$$\tau = 145.1\text{fs} (6000\text{a.u.})$$

Time step:

$$24.19\text{as} (1\text{a.u.})$$

Stohr, *NEXAFS Spectroscopy*

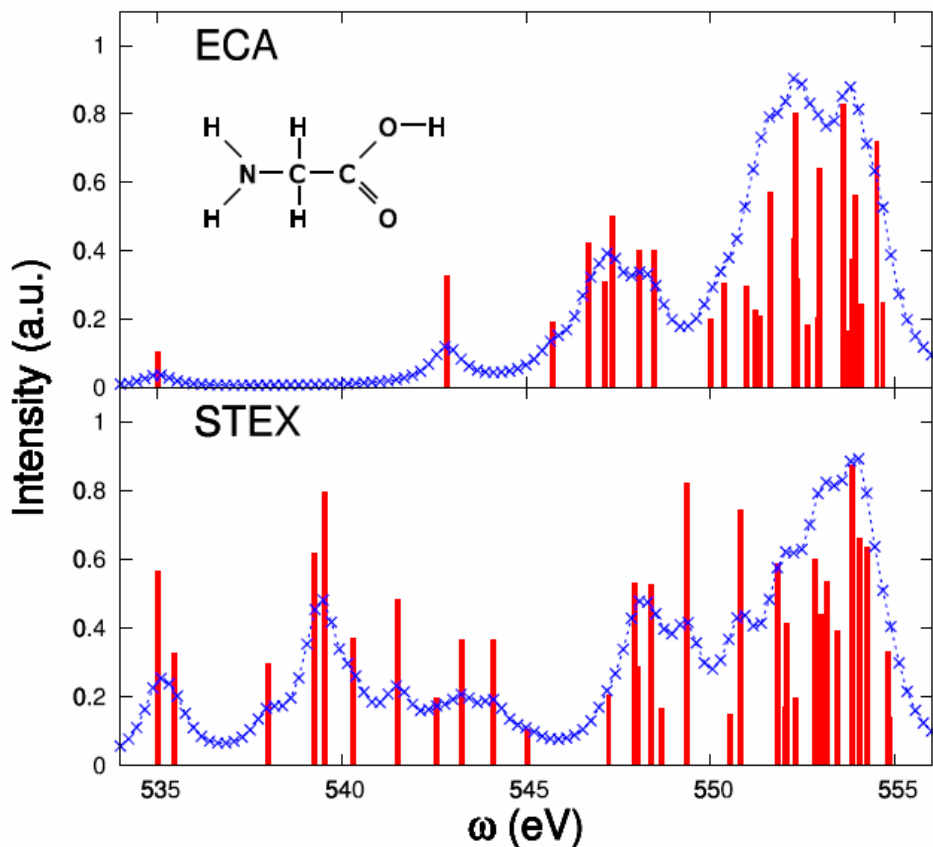
$$\begin{aligned} |f\rangle &= \sum_{ia} C_i^a c_a^\dagger c_i |g\rangle \\ D_{f;ia} &= D_f \times C_i^a \\ W_{f;ia} &= W_f \times C_i^a \end{aligned}$$

# XANES Spectra

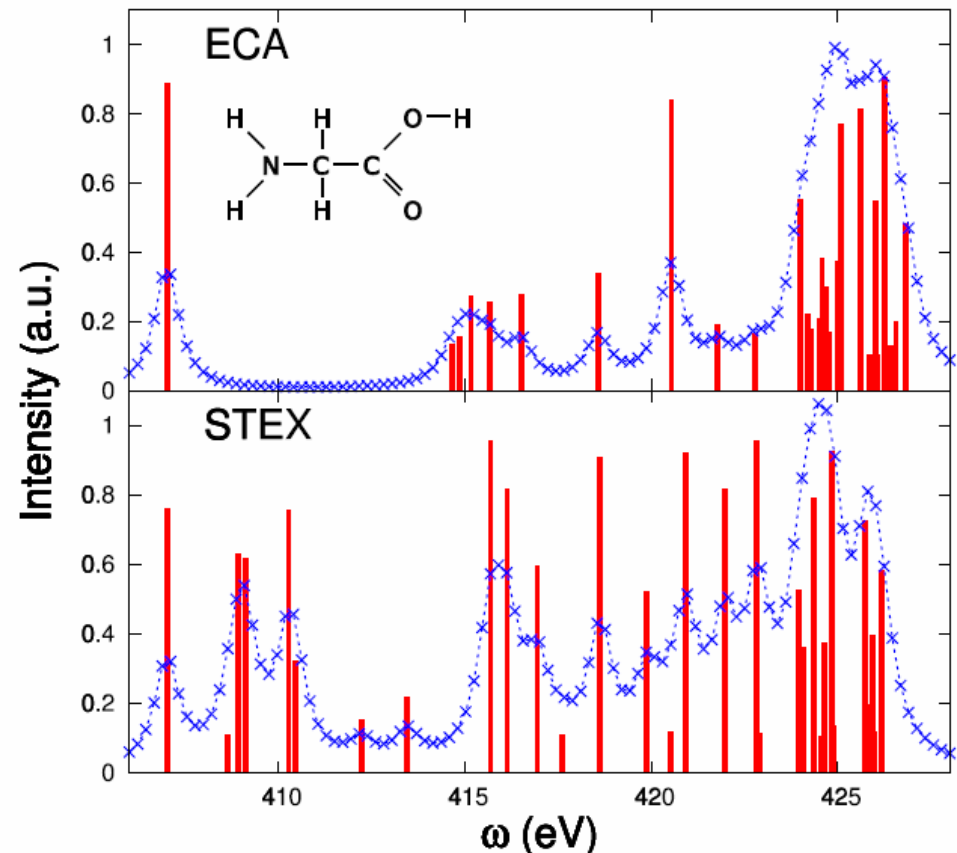
STEX reports additional XANES peaks due to improved unoccupied orbitals.

$$S_{XANES}(\omega) = \frac{1}{\pi} \sum_f |\mu_{fg}| \frac{\gamma_f^2}{(\omega - \omega_{fg})^2 + \gamma_f^2}$$

Oxygen



Nitrogen





# CXRS Signal

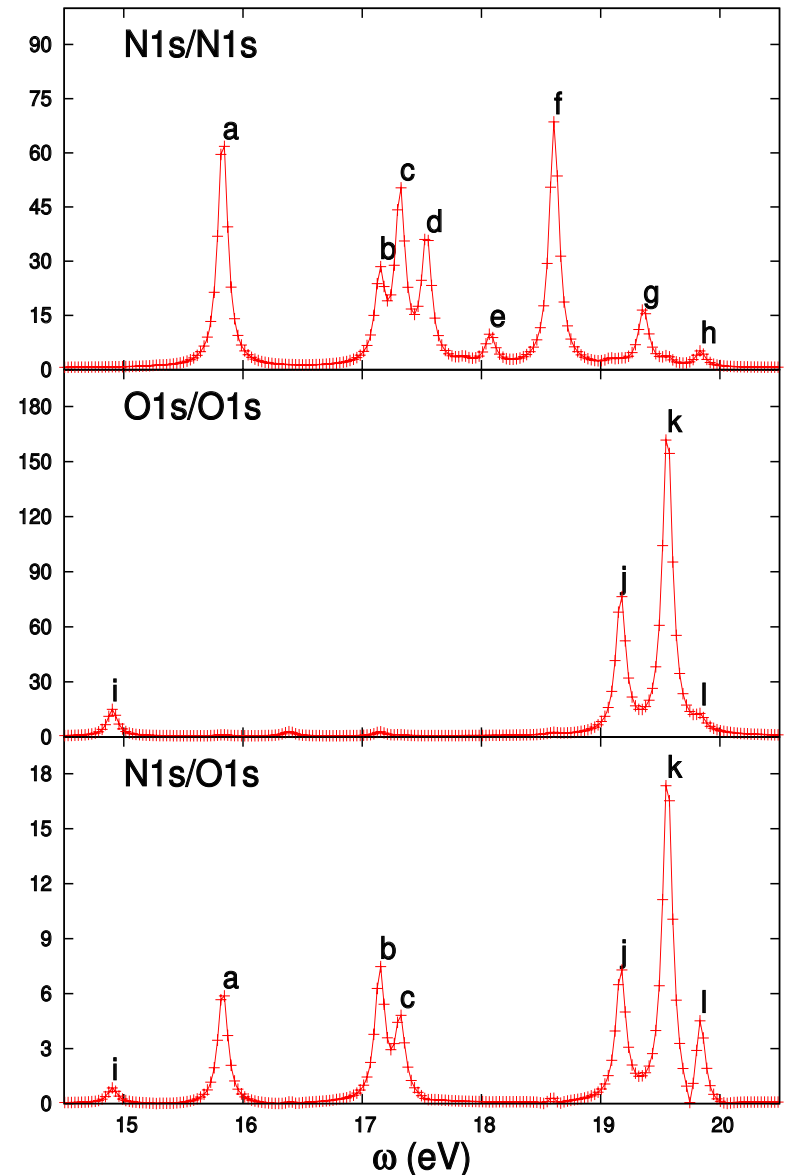
$$|D(\tau)\rangle = \sum_{f,ia} e^{-i\omega_{fg}\tau - \gamma_f\tau} D_{f;ia} c_a^\dagger c_i |g\rangle |W\rangle = \sum_{f,ia} W_{f;ia} c_a^\dagger c_i |g\rangle$$

N1s doorway at time  $t=0$  ( $i, a$ : relaxed orbitals)

	$\omega_{fg}(eV)$	$D_{f;ia}$	$i$	$a$
$a$	15.83	0.49	HOMO	LUMO+2
$b$	17.15	0.29	HOMO-2	LUMO
$c$	17.32	0.42	HOMO-1	LUMO+1
$d$	17.54	0.36	HOMO-2	LUMO+1
$e$	18.07	0.17	HOMO-2	LUMO+2
$f$	18.61	0.49	HOMO-2	LUMO+3
$g$	19.36	0.24	HOMO-2	LUMO+4
$h$	19.84	0.12	HOMO-2	LUMO+5

O1s window

	$\omega_{fg}(eV)$	$W_{f;ia}$	$i$	$a$
$i$	14.90	0.23	HOMO	LUMO
$j$	19.17	0.53	HOMO-3	LUMO
$k$	19.56	0.79	HOMO-3	LUMO+1
$l$	19.84	-0.15	HOMO-2	LUMO+5



# Visualization of Electron Dynamics

Molecular orbital representation is good for assigning CXRS peaks. But to visualize the wave packet evolution, it requires to monitor all the particle-hole pairs that contribute to the signal.

$$|D(\tau)\rangle = \sum_{f,ia} e^{-i\omega_{fg}\tau - \gamma_f\tau} D_{f;ia} c_a^\dagger c_i |g\rangle$$

$$|W\rangle = \sum_{f,ia} W_{f;ia} c_a^\dagger c_i |g\rangle$$

In fact, there are no dominant particle-hole pairs that contribute to the signal in the molecular orbital basis. To visualize the electron dynamics, we choose natural transition orbital representation, which provides a more compact representation.

## References:

E. Schmidt, Math. Ann., 63:433 (1907)

A. T. Amos and G. G. Hall, Proc. R. Soc. Lond. A, 263:483 (1961)

R. L. Martin, JCP, 118:4775 (2003)

the window matrix and the signal are also expanded in terms of these orbitals

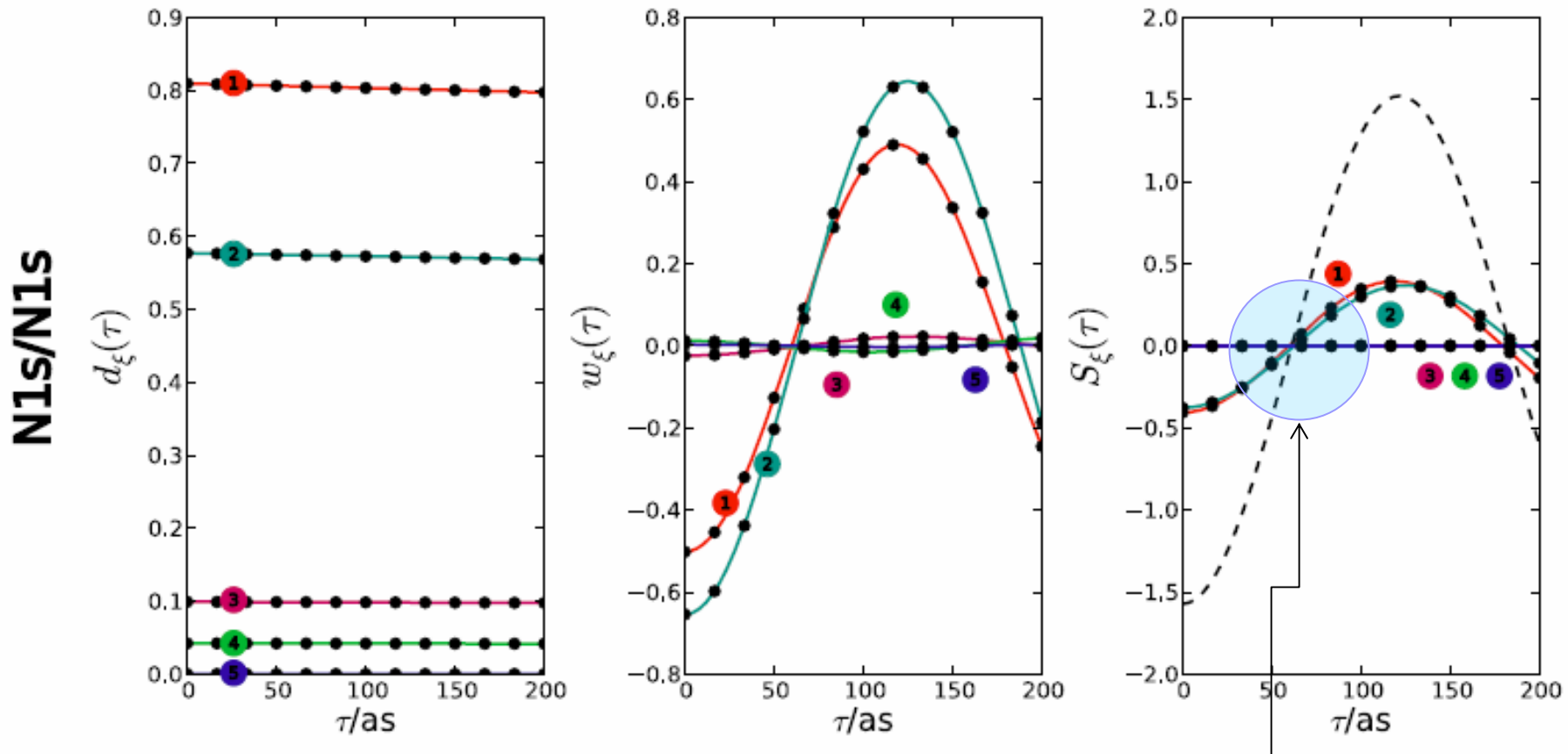
$$\begin{aligned}
 S(\tau) &= 2\text{Re Tr} [\mathbf{W}^T \mathbf{D}(\tau)] \\
 &= 2\text{Re Tr} [\mathbf{W}^T \mathbf{X}^p(\tau) \mathbf{X}^{p\dagger}(\tau) \mathbf{D} \mathbf{X}^h(\tau) \mathbf{X}^{h\dagger}(\tau)] \\
 &= 2\text{Re} \sum_{\xi} w_{\xi}(\tau) d_{\xi}(\tau)
 \end{aligned}$$

where the time-dependent doorway and window natural orbital weights are defined as

$$\begin{aligned}
 w_{\xi}(\tau) &= \sum_{ai} \chi_{\xi i}^h W_{ia}^* e^{-\omega_{ai}\tau} \chi_{a\xi}^p \\
 d_{\xi}(\tau) &= \sum_{ai} \chi_{a\xi}^{p*} D_{ai} \chi_{\xi i}^{h*} e^{-\Gamma_{ai}\tau}
 \end{aligned}$$

Signal is now expressed as a weighted sums of products, each representing the contribution of a single natural orbital

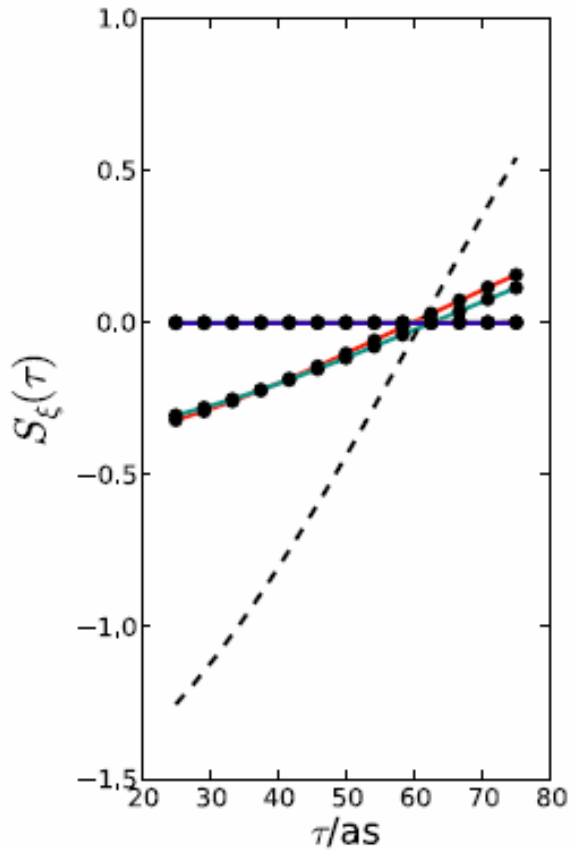
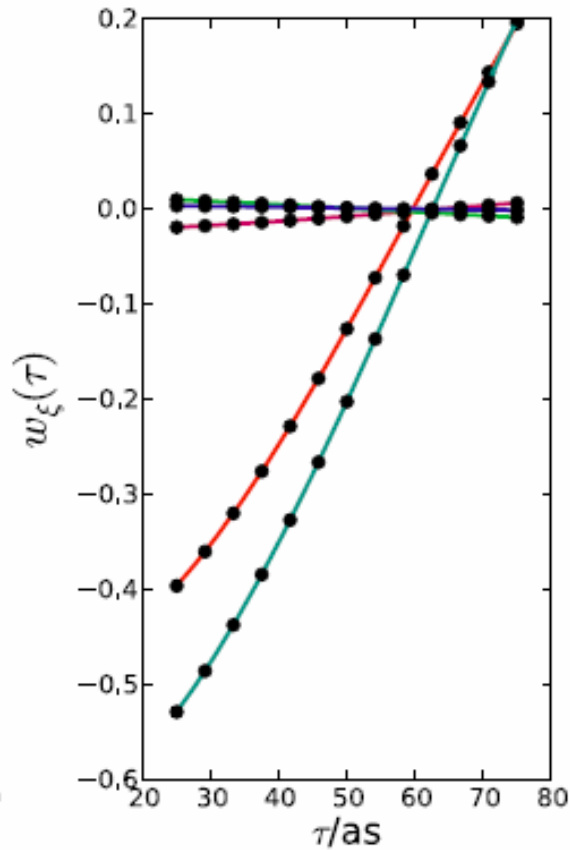
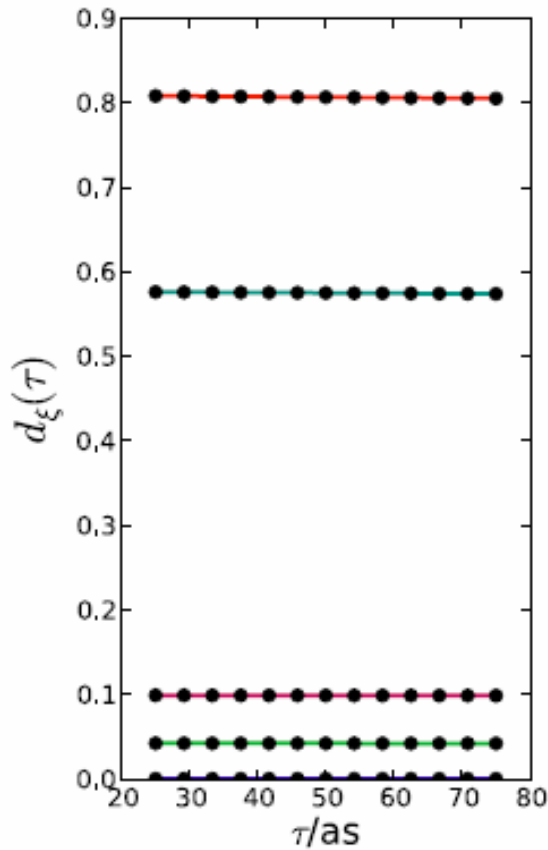
# Signal decomposition by natural orbital pair



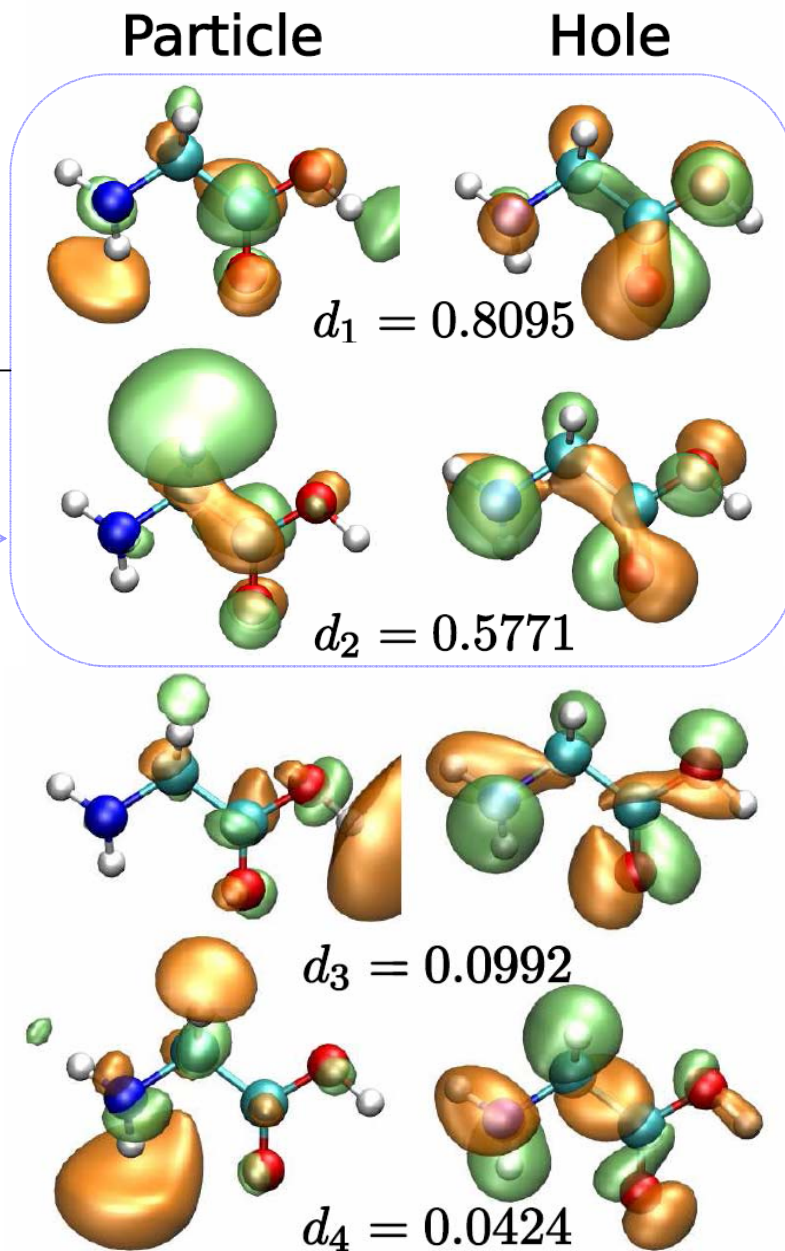
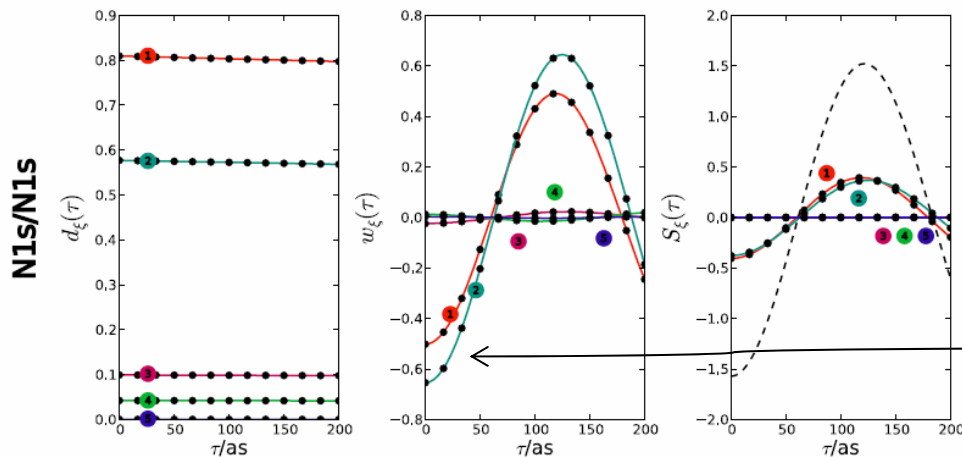
Pulse width:  $\sigma_j = 77as(1/\sigma_j \simeq 10eV)$

zooming in on the crossing...

**NIS/NIS**



**for this system, the dominant contribution comes from the natural orbitals with the strongest doorway weights**



Natural Orbitals at

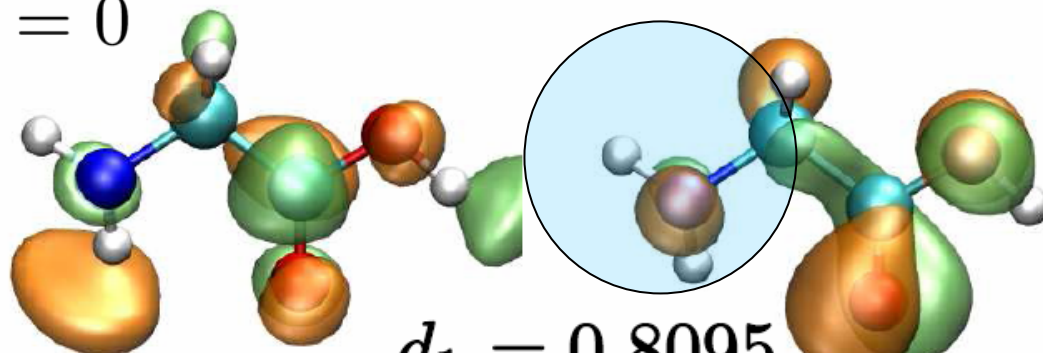
$$\tau = 0$$

The strongest contribution is from the first two natural orbitals.

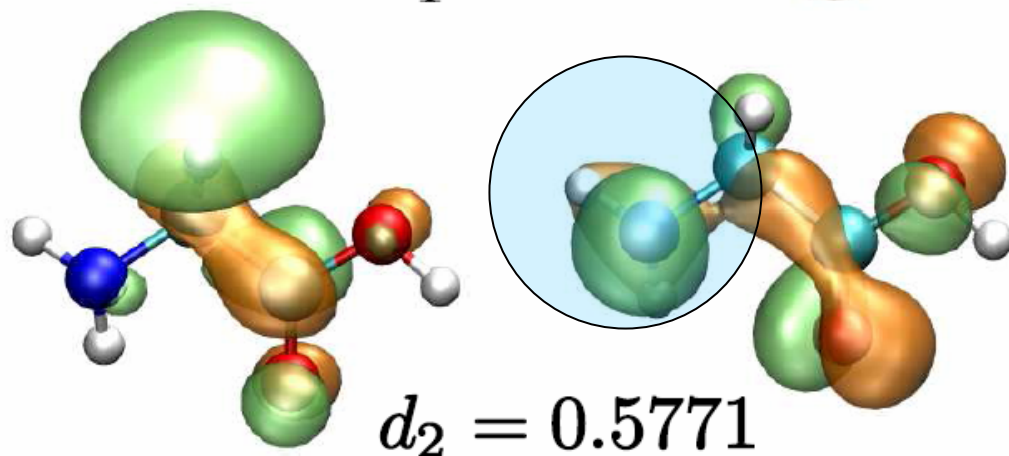
Particle

Hole

$$\tau = 0$$



$$d_1 = 0.8095$$



$$d_2 = 0.5771$$

**Selection rule:** x-ray dipole is strong between s type core-orbitals, and valence orbitals with a strong projection onto the p-orbitals local to the resonant core.

both of the natural orbitals contributing strongly to the signal contain p-orbital character in their hole natural orbitals.

# Spatial Representation of Natural Orbitals

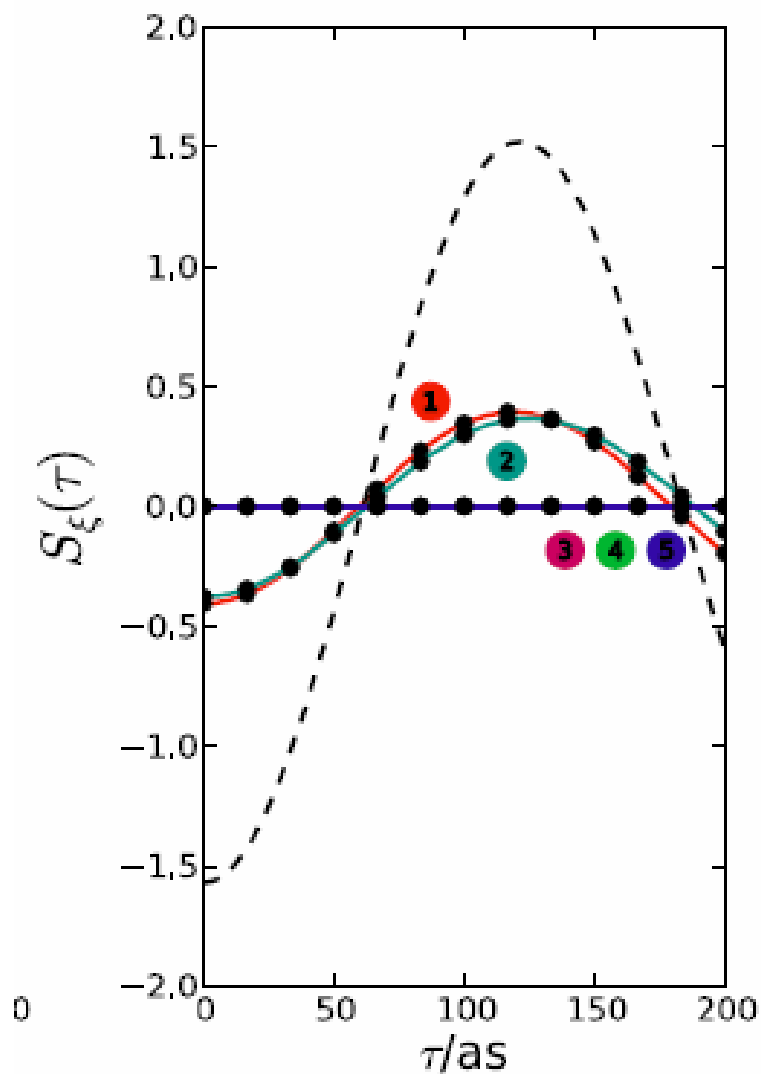
The natural orbitals can be expanded in the atomic basis functions of the signal

$$\phi_{p,\xi}^*(r, \tau) = \sum_{a\alpha} \chi_{a\xi}^p C_{a\alpha} \phi_{\alpha}^*(r) e^{-i\varepsilon_a \tau}$$

$$\phi_{h,\xi}(r, \tau) = \sum_{i\beta} \chi_{\xi i}^h C_{i\beta}^* \phi_{\beta}(r) e^{i\varepsilon_i \tau}$$

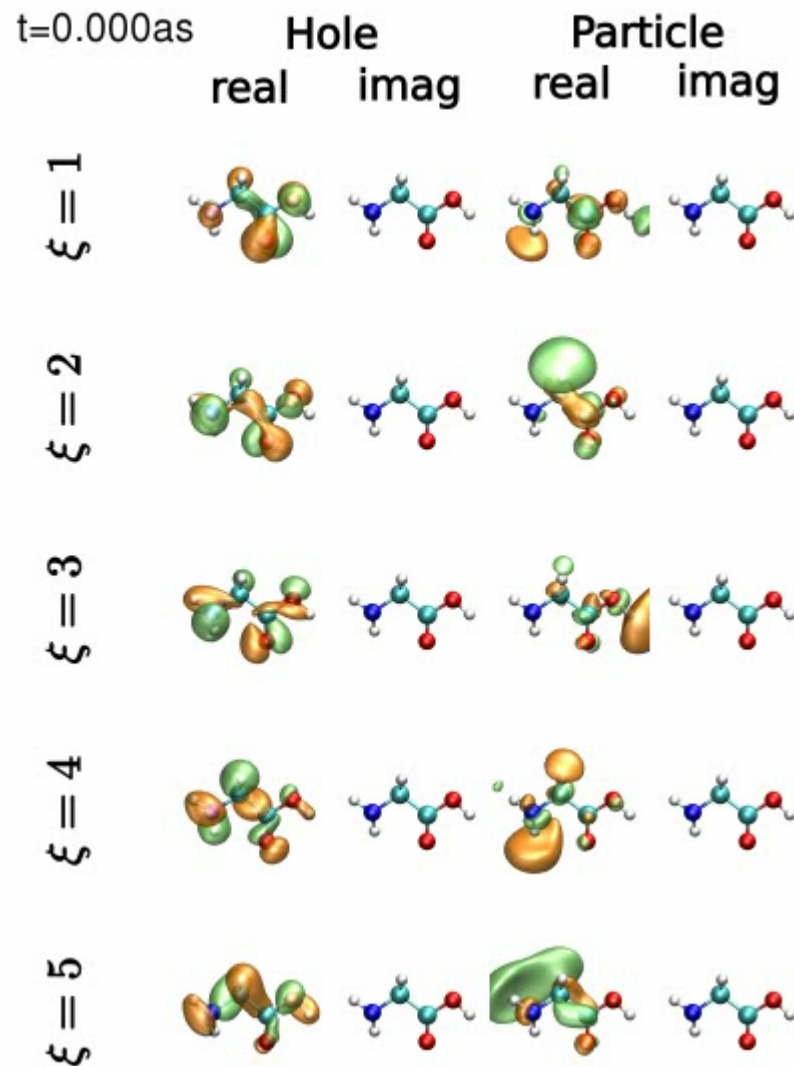


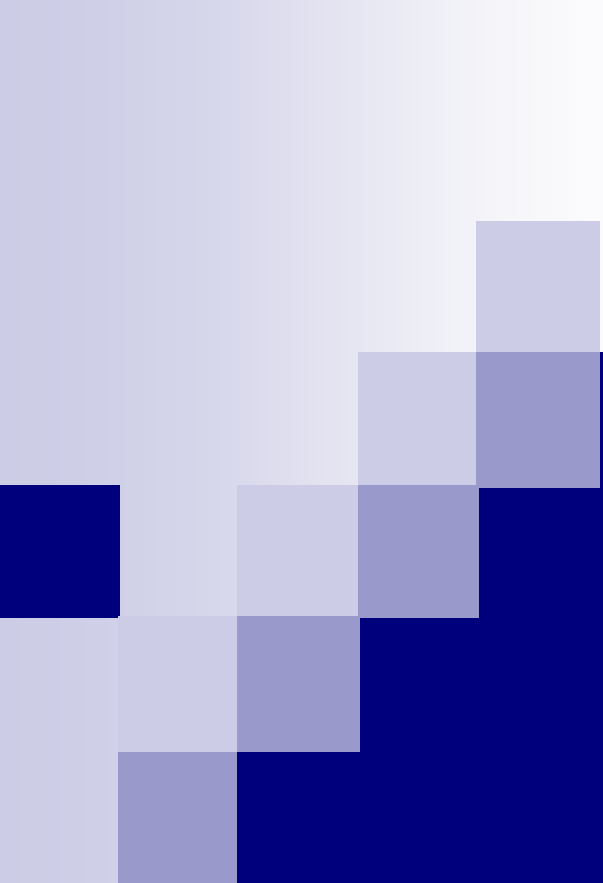
# Time-dependent Natural Orbitals



Time: 0as – 200as

Time-dependent Natural Orbitals



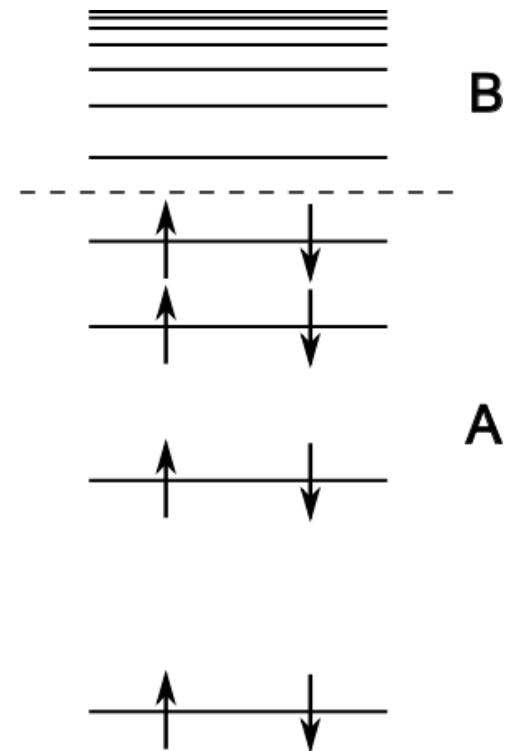
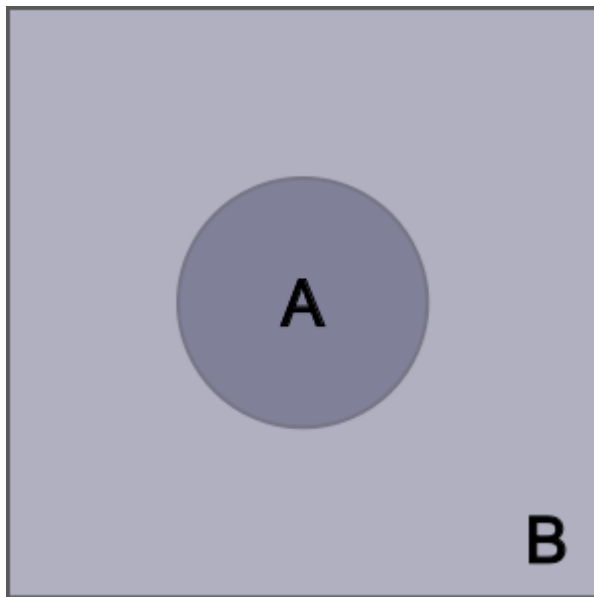


**Manipulating Quantum  
Entanglement of Quasiparticles  
in Many-Electron Systems  
by Attosecond X-ray Pulses**

**Shaul Mukamel and  
Haitao Wang**

Department of Chemistry,  
University of California, Irvine

# Entanglement: concurrence



# Concurrence

Reduced density matrix:

$$\sigma_e = \text{Tr}_h |\psi\rangle\langle\psi| = S^\dagger S \quad \sigma_h = \text{Tr}_e |\psi\rangle\langle\psi| = S S^\dagger$$

Schmidt representation diagonalizes both  $\sigma_e$  and  $\sigma_h$  simultaneously, sharing  $d$  non-zero eigenvalues  $\lambda_\nu$  with  $\nu = 1, 2, \dots, d$ .

$$|\psi(t)\rangle = \sum_{\nu=1}^d \sqrt{\lambda_\nu(t)} c_\nu^\dagger d_\nu^\dagger |g\rangle$$

Participation ratio  $R^{-1}$  with  $R = \text{Tr} \sigma_e^2 = \sum_{\nu} \lambda_\nu^2$  measures the number of electron-hole pairs participating in the wave packet.

Concurrence  $C = \sqrt{2(1 - R)} = \sqrt{\sum_{\nu < \nu'} \lambda_\nu \lambda_{\nu'}}$  is another measure of entanglement commonly used in quantum information applications.

# Simulation results: carbon monoxide (CO)

- Geometry optimized at B3LYP/6-311G\*\* level.
- Excitation energies and transition dipole moments calculated with the minimal basis STO-3G basis set.
- Line-width:  $\Gamma_f = 0.5eV$  and broadband width:  $\sigma_1 = 20eV$

$ g'\rangle$	$\omega_{g'g}$ (eV)	$ D_{g'} ^2$ (oxygen K-edge)	$ D_{g'} ^2$ (carbon K-edge)	$ D_{g'} ^2$ ( $\sigma_1 \rightarrow \pi^*$ )
4	10.69	0.03796	0.01182	0.00905
5	10.69	<b>0.06269</b>	0.01953	0.01495
8	19.56	<b>0.06073</b>	<b>0.37849</b>	<b>0.44332</b>
11	31.68	<b>0.68598</b>	<b>0.58300</b>	<b>0.11670</b>
14	36.50	<b>0.15025</b>	0.00051	<b>0.38921</b>
15	55.53	0.00240	0.00665	0.02677

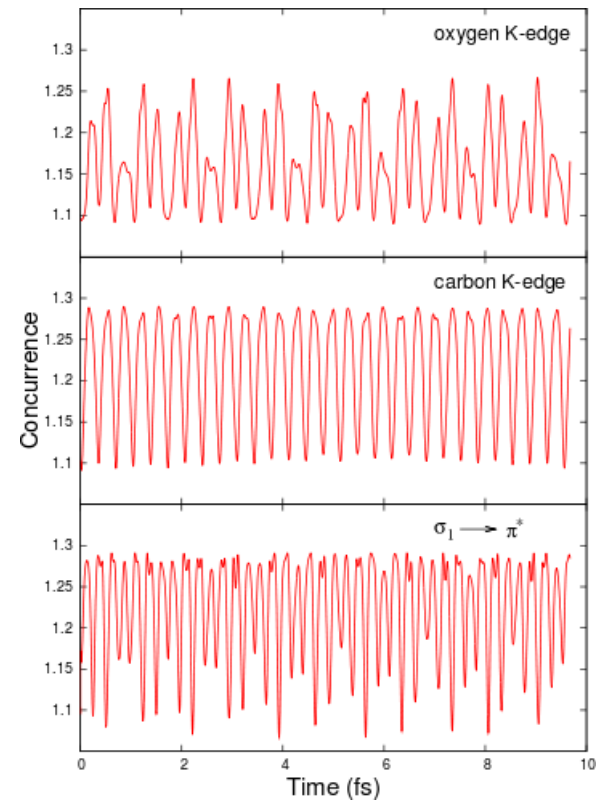
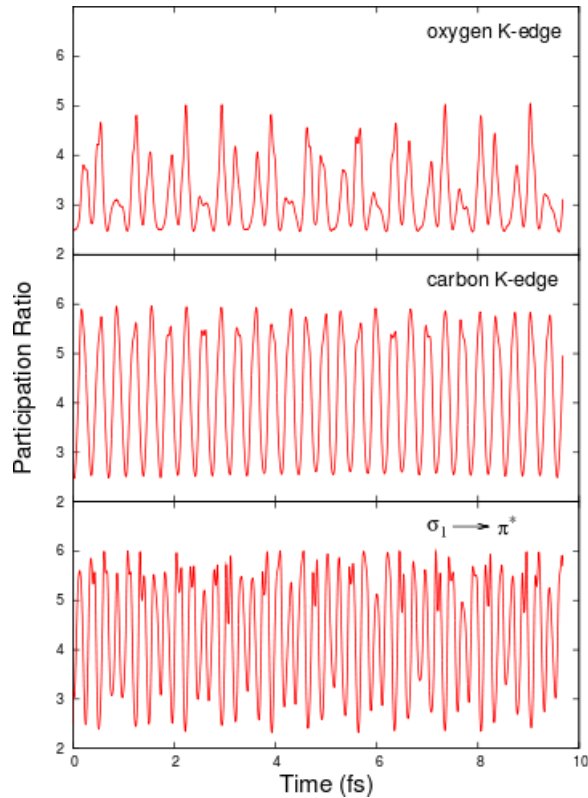
Table: The 6 major valence-excited state contributions to the valence wave packets prepared by the three core transitions used in the present simulations. The states are labeled in increasing order of energies (column 1).

# Simulation results: carbon monoxide (CO)

For a given  $d$ , the concurrence has a maximum value of  $C_{max} = \sqrt{2(1 - 1/d)}$ .

$$2 < d < 6$$

$$C_{max} = \begin{cases} 1.00 & d = 2 \\ 1.29 & d = 6 \end{cases}$$



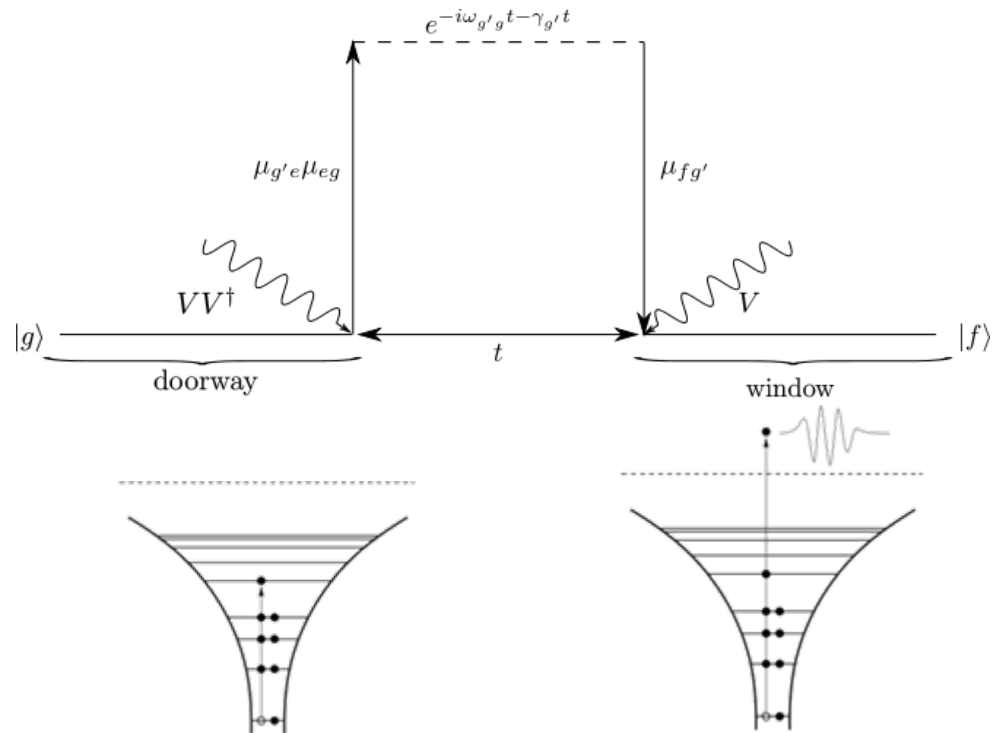
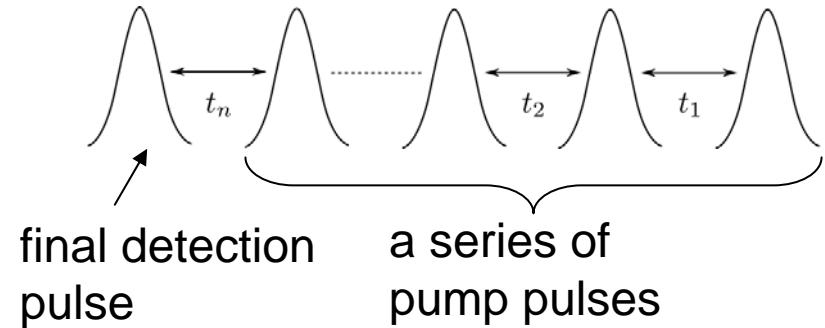


# Multidimensional Attosecond Photoelectron Spectroscopy

Shaul Mukamel, Haitao Wang ,  
Saar Rahav  
University of California, Irvine

# Multidimensional Attosecond Photoelectron Spectroscopy

- Well-separated pulses
- Detection pulse interacts with the molecule once, ionizes the molecule, and generates a photoelectron.
- The signal is the number of photoelectron with kinetic energy  $\mathcal{E}_{\mathbf{k}}$ .





# Photoelectron Signal in Frequency Domain

The signal is a square modulus of transition amplitude evaluated at the transition frequency.

$$\begin{aligned}\tilde{S}(\varepsilon) &= \hbar^{-2} \int d\omega |T_{fg}(\omega)|^2 \rho_f(\varepsilon) \delta(\omega - \omega_{f,g}) \\ &= \hbar^{-2} |T_{fg}(\omega_{fg})|^2 \rho_f(\varepsilon)\end{aligned}$$

where  $\varepsilon_f^- + \varepsilon - \varepsilon_g = \hbar\omega_{fg}$  ← transition energy

↑ internal energy of the ion state      kinetic energy of the photoelectron      internal energy of the neutral state

The transition amplitude can be expanded in powers of various pulses:

$$\begin{aligned}T_{fg}(\omega) &= \int d\omega_1 E^d(\omega_1) \tilde{T}_{fg}^{(1)}(\omega_1) \delta(\omega - \omega_1) \\ &+ (2\pi\hbar)^{-1} \int d\omega_1 d\omega_2 E^p(\omega_1) E^d(\omega_2) \tilde{T}_{fg}^{(2)}(\omega_2, \omega_1) \delta(\omega - \omega_1 - \omega_2) \\ &+ (2\pi\hbar)^{-2} \int d\omega_1 d\omega_2 d\omega_3 E^p(\omega_1) E^p(\omega_2) E^d(\omega_3) \tilde{T}_{fg}^{(3)}(\omega_3, \omega_2, \omega_1) \delta(\omega - \omega_1 - \omega_2 - \omega_3) + \dots\end{aligned}$$